(2003). Mutations in the DJ-1 gene associated with autosomal recessive early-onset parkinsonism. *Science*, **299**: 256-259.

Carey, R.J., Pinheiro-Carrera, M., Dai, H., Tomaz, C., and Huston, J.P. (1995). L-DOPA and psychosis: evidence for L-DOPA-induced increases in prefrontal cortex dopamine and in serum corticosterone. *Biol Psychiatry*, **38**: 669-676.

Chang, J.W., Wachtel, S.R., Young, D., and Kang, U.J. (1999). Biochemical and anatomical characterization of forepaw adjusting steps in rat models of Parkinson's disease: studies on medial forebrain bundle and striatal lesions. *Neuroscience*, **88**: 617-628.

Chiorini, J.A., Yang, L., Liu, Y., Safer, B., and Kotin, R.M. (1997). Cloning of adeno-associated virus type 4 (AAV4) and generation of recombinant AAV4 particles. *J Virol*, **71**: 6823-6833.

Chiorini, J.A., Kim, F., Yang, L., and Kotin, R.M. (1999). Cloning and characterization of adeno-associated virus type 5. *J Virol*, **73**: 1309-1319.

Choi-Lundberg, D.L., Lin, Q., Chang, Y.N., Chiang, Y.L., Hay, C.M., Mohajeri, H., Davidson, B.L., and Bohn, M.C. (1997). Dopaminergic neurons protected from degeneration by GDNF gene therapy. *Science*, **275**: 838-841.

Connor, B., Kozlowski, D.A., Schallert, T., Tillerson, J.L., Davidson, B.L., and Bohn, M.C. (1999). Differential effects of glial cell line-derived neurotrophic factor (GDNF) in the striatum and substantia nigra of the aged Parkinsonian rat. *Gene Ther*, **6**: 1936-1951.

Connor, B., Kozlowski, D.A., Unnerstall, J.R., Elsworth, J.D., Tillerson, J.L., Schallert, T., and Bohn, M.C. (2001). Glial cell line-derived neurotrophic factor (GDNF) gene delivery protects dopaminergic terminals from degeneration. *Exp Neurol*, **169**: 83-95.

Cookson, M.R. (2003). Pathways to parkinsonism. *Neuron*, **37**: 7-10.

Deumens, R., Blokland, A., and Prickaerts, J. (2002). Modeling Parkinson's disease in rats: an evaluation of 6-OHDA lesions of the nigrostriatal pathway. *Exp Neurol*, **175**: 303-317.

Dunnett, S.B., and Bjorklund, A. (1999). Prospects for new restorative and neuroprotective treatments in Parkinson's disease. *Nature*, **399**: A32-39.

Elliott, J.L. (1999). Experimental models of amyotrophic lateral sclerosis. *Neurobiol Dis*, **6**: 310-320.

Forno, L.S., Langston, J.W., Delanney, L.E., Irwin, I., and Ricaurte, G.A. (1986). Locus ceruleus lesions and eosinophilic inclusions in MPTP-treated monkeys. *Ann Neurol*, **20**: 449-455.

Gao, G.P., Alvira, M.R., Wang, L., Calcedo, R., Johnston, J., and Wilson, J.M. (2002). Novel adeno-associated viruses from rhesus monkeys as vectors for human gene therapy. *Proc Natl Acad Sci U S A*, **99**: 11854-11859.

Gurney, M.E., Pu, H., Chiu, A.Y., Dal Canto, M.C., Polchow, C.Y., Alexander, D.D., Caliendo, J., Hentati, A., Kwon, Y.W., Deng, H.X., and *Et al.* (1994). Motor neuron degeneration in mice that express a human Cu,Zn superoxide dismutase mutation. *Science*, **264**: 1772-1775.

Gwinn-Hardy, K. (2002). Genetics of parkinsonism. *Mov Disord*, **17**: 645-656.

Hadano, S., Hand, C.K., Osuga, H., Yanagisawa, Y., Otomo, A., Devon, R.S., Miyamoto, N., Showguchi-Miyata, J., Okada, Y., Singaraja, R., Figlewicz, D.A., Kwiatkowski, T., Hosler, B.A., Sagie, T., Skaug, J., Nasir, J., Brown, R.H., Jr., Scherer, S.W., Rouleau, G.A., Hayden, M.R. and Ikeda, J.E. (2001). A gene encoding a putative GTPase regulator is mutated in familial amyotrophic lateral sclerosis 2. *Nat Genet*, **29**: 166-173.

Hoshiga, M., Hatakeyama, K., Watanabe, M., Shimada, M., and Kagamiyama, H. (1993). Autoradiographic distribution of [14C]tetrahydrobiopterin and its developmental change in mice. *J Pharmacol Exp Ther*, **267**: 971-978.

Jenner, P. (2000). Factors influencing the onset and persistence of dyskinesia in MPTP-treated primates. *Ann Neurol*, **47**: S90-99.

Kaddis, F.G., Clarkson, E.D., Weber, M.J., Vandenbergh, D.J., Donovan, D.M., Mallet, J., Horellou, P., Uhl, G.R., and Freed, C.R. (1997). Intrastriatal grafting of Cos cells stably expressing human aromatic L-amino acid decarboxylase: neurochemical effects. *J Neurochem*, **68**: 1520-1526.

Kaludov, N., Handelman, B., and Chiorini, J.A. (2002). Scalable purification of adeno-associated virus type 2, 4, or 5 using ion-exchange chromatography. *Hum Gene Ther*, **13**: 1235-43.

Kirik, D., Rosenblad, C., Bjorklund, A., and Mandel, R.J. (2000). Long-term rAAV-mediated gene transfer of GDNF in the rat Parkinson's model: intrastriatal but not intranigral transduction promotes functional regeneration in the lesioned nigrostriatal system. *J Neurosci*, **20**: 4686-4700.

Kish, S.J., Shannak, K., and Hornykiewicz, O. (1988). Uneven pattern of dopamine loss in the striatum of patients with idiopathic Parkinson's disease. Pathophysiologic and clinical implications. *N Engl J Med*, **318**: 876-880.

Kitada, T., Asakawa, S., Hattori, N., Matsumine, H., Yamamura, Y., Minoshima, S., Yokochi, M., Mizuno, Y., and Shimizu, N. (1998). Mutations in the parkin gene cause autosomal recessive juvenile parkinsonism. *Nature*, **392**: 605-608.

Kordower, J.H., Palfi, S., Chen, E.Y., Ma, S.Y., Sendera, T., Cochran, E.J., Mufson, E.J., Penn, R., Goetz, C.G., and Comella, C.D. (1999). Clinicopathological findings following intraventricular glial-derived neurotrophic factor treatment in a patient with Parkinson's disease. *Ann Neurol*, **46**: 419-424.

Kordower, J.H., Emborg, M.E., Bloch, J., Ma, S.Y., Chu, Y., Leventhal, L., Mcbride, J., Chen, E.Y., Palfi, S., Roitberg, B.Z., Brown, W.D., Holden, J.E., Pyzalski, R., Taylor, M.D., Carvey, P., Ling, Z., Trono, D., Hantraye, P., Deglon, N., and Aebischer, P. (2000). Neurodegeneration prevented by lentiviral vector delivery of GDNF in primate models of Parkinson's disease. *Science*, **290**: 767-773.

Kowall, N.W., Hantraye, P., Brouillet, E., Beal, M.F., Mckee, A.C., and Ferrante, R.J. (2000). MPTP induces alpha-synuclein aggregation in the substantia nigra of baboons. *Neuroreport*, **11**: 211-213.

Kozlowski, D.A., Connor, B., Tillerson, J.L., Schallert, T., and Bohn, M.C. (2000). Delivery of a GDNF gene into the substantia nigra after a progressive 6- OHDA lesion maintains functional nigrostriatal connections. *Exp Neurol*, **166**: 1-15.

Langston, J.W., Quik, M., Petzinger, G., Jakowec, M., and Di Monte, D.A. (2000). Investigating levodopa-induced dyskinesias in the parkinsonian primate. *Ann Neurol*, **47**: S79-89.

Lee, C.S., Sauer, H., and Bjorklund, A. (1996). Dopaminergic neuronal degeneration and motor impairments following axon terminal lesion by instrastriatal 6-hydroxydopamine in the rat. *Neuroscience*, **72**: 641-653.

Leroy, E., Boyer, R., Auburger, G., Leube, B., Ulm, G., Mezey, E., Harta, G., Brownstein, M.J., Jonnalagada, S., Chernova, T., Dehejia, A., Lavedan, C., Gasser, T., Steinbach, P.J., Wilkinson, K.D., and Polymeropoulos, M.H. (1998). The ubiquitin pathway in Parkinson's disease. *Nature*, **395**: 451-452.

Lu, Y.Y., Wang, L.J., Muramatsu, S., Ikeguchi, K., Fujimoto, K., Okada, T., Mizukami, H., Matsushita, T., Hanazono, Y., Kume, A., Nagatsu, T., Ozawa, K., and Nakano, I. (2003). Intramuscular injection of AAV-GDNF results in sustained expression of transgenic GDNF, and its delivery to spinal motoneurons by retrograde transport. *Neurosci Res*, **45**: 33-40.

Mandel, R.J., Spratt, S.K., Snyder, R.O., and Leff, S.E. (1997). Midbrain injection of recombinant adeno-associated virus encoding rat glial cell line-derived neurotrophic factor protects nigral neurons in a progressive 6-hydroxydopamine-induced degeneration model of Parkinson's disease in rats. *Proc Natl Acad Sci U S A*, **94**: 14083-14088.

Mandel, R.J., Snyder, R.O., and Leff, S.E. (1999). Recombinant adeno-associated viral vector-mediated glial cell line-derived neurotrophic factor gene transfer protects nigral dopamine neurons after onset of progressive degeneration in a rat model of Parkinson's disease. *Exp Neurol*, **160**: 205-214.

Matsushita, T., Elliger, S., Elliger, C., Podsakoff, G., Villarreal, L., Kurtzman, G.J., Iwaki, Y., and Colosi, P. (1998). Adeno-associated virus vectors can be efficiently produced without helper virus. *Gene Ther*, **5**: 938-945.

Monahan, P.E., and Samulski, R.J. (2000). AAV vectors: is clinical success on the horizon? *Gene Ther*, **7**: 24-30.

Muramatsu, S., Mizukami, H., Young, N.S., and Brown, K.E. (1996). Nucleotide sequencing and generation of an infectious clone of adeno-associated virus 3. *Virology*, **221**: 208-217.

Muramatsu, S., Fujimoto, K., Ikeguchi, K., Shizuma, N., Kawasaki, K., Ono, F., Shen, Y., Wang, L., Mizukami, H., Kume, A., Matsumura, M., Nagatsu, I., Urano, F., Ichinose, H., Nagatsu, T., Terao, K., Nakano, I., and Ozawa, K. (2002). Behavioral recovery in a primate model of Parkinson's disease by triple transduction of striatal cells with adeno-associated viral vectors expressing dopamine-synthesizing enzymes. *Hum Gene Ther*, **13**: 345-354.

Nagatsu, T., and Ichinose, H. (1999). Regulation of pteridine-requiring enzymes by the cofactor tetrahydrobiopterin. *Mol Neurobiol*, **19**: 79-96.

Nagatsu, T., Horikoshi, T., Sawada, M., Nagatsu, I., Kondo, T., Iizuka, R., and Narabayashi, H. (1987). Biosynthesis of tetrahydrobiopterin in parkinsonian human brain. *Adv Neurol*, **45**: 223-226.

Nagatsu, I., Arai, R., Sakai, M., Yamawaki, Y., Takeuchi, T., Karasawa, N. and Nagatsu,

T. (1997). Immunohistochemical colocalization of GTP cyclohydrolase I in the nigrostriatal system with tyrosine hydroxylase. *Neurosci Lett*, **224**: 185-188.

Nakamura, K., Ahmed, M., Barr, E., Leiden, J.M., and Kang, U.J. (2000). The localization and functional contribution of striatal aromatic L-amino acid decarboxylase to L-3,4-dihydroxyphenylalanine decarboxylation in rodent parkinsonian models. *Cell Transplant*, **9**: 567-576.

Natsume, A., Mata, M., Goss, J., Huang, S., Wolfe, D., Oligino, T., Glorioso, J., and Fink, D.J. (2001). Bcl-2 and GDNF delivered by HSV-mediated gene transfer act additively to protect dopaminergic neurons from 6-OHDA-induced degeneration. *Exp Neurol*, **169**: 231-238.

Olanow, C.W., Watts, R.L. and Koller, W.C. (2001). An algorithm (decision tree) for the management of Parkinson's disease: treatment guidelines. *Neurology*, **56**: S1-S88.

Polymeropoulos, M.H., Lavedan, C., Leroy, E., Ide, S.E., Dehejia, A., Dutra, A., Pike, B., Root, H., Rubenstein, J., Boyer, R., Stenroos, E.S., Chandrasekharappa, S., Athanassiadou, A., Papapetropoulos, T., Johnson, W.G., Lazzarini, A.M., Duvoisin, R.C., Di Iorio, G., Golbe, L.I., and Nussbaum, R.L. (1997). Mutation in the alpha-synuclein gene identified in families with Parkinson's disease. *Science*, **276**: 2045-2047.

Raoul, C., Estevez, A.G., Nishimune, H., Cleveland, D.W., Delapeyriere, O., Henderson, C.E., Haase, G., and Pettmann, B. (2002). Motoneuron death triggered by a specific pathway downstream of Fas. potentiation by ALS-linked SOD1 mutations. *Neuron*, **35**: 1067-1083.

Rosen, D.R., Siddique, T., Patterson, D., Figlewicz, D.A., Sapp, P., Hentati, A., Donaldson, D., Goto, J., O'regan, J.P., Deng, H.X., and *Et al.* (1993). Mutations in Cu/Zn superoxide dismutase gene are associated with familial amyotrophic lateral sclerosis. *Nature*, **362**: 59-62.

Rutledge, E.A., Halbert, C.L., and Russell, D.W. (1998). Infectious clones and vectors derived from adeno-associated virus (AAV) serotypes other than AAV type 2. *J Virol*, **72**: 309-319.

Shen, Y., Muramatsu, S., Ikeguchi, K., Fujimoto, K., Fan, D.S., Ogawa, M., Mizukami, H., Urabe, M., Kume, A., Nagatsu, I., Urano, F., Suzuki, T., Ichinose, H., Nagatsu, T., Monahan, J., Nakano, I., and Ozawa, K. (2000). Triple transduction with adeno-associated virus vectors expressing tyrosine hydroxylase, aromatic-L-amino-acid decarboxylase, and GTP cyclohydrolase I for gene therapy of Parkinson's disease. *Hum Gene Ther*, **11**: 1509-1519.

Speciale, S.G. (2002). MPTP: insights into parkinsonian neurodegeneration. *Neurotoxicol Teratol*, **24**: 607-620.

Srivastava, A., Lusby, E.W., and Berns, K.I. (1983). Nucleotide sequence and organization of the adeno-associated virus 2 genome. *J Virol*, **45**: 555-564.

Tillerson, J.L., Cohen, A.D., Philhower, J., Miller, G.W., Zigmond, M.J., and Schallert, T. (2001). Forced limb-use effects on the behavioral and neurochemical effects of 6-hydroxydopamine. *J Neurosci*, **21**: 4427-4435.

Wang, L., Muramatsu, S., Lu, Y., Ikeguchi, K., Fujimoto, K., Okada, T., Mizukami,

H., Hanazono, Y., Kume, A., Urano, F., Ichinose, H., Nagatsu, T., Nakano, I., and Ozawa, K. (2002a). Delayed delivery of AAV-GDNF prevents nigral neurodegeneration and promotes functional recovery in a rat model of Parkinson's disease. *Gene Ther*, **9**: 381-389.

Wang, L.J., Lu, Y.Y., Muramatsu, S., Ikeguchi, K., Fujimoto, K., Okada, T., Mizukami, H., Matsushita, T., Hanazono, Y., Kume, A., Nagatsu, T., Ozawa, K., and Nakano, I. (2002b). Neuroprotective effects of glial cell line-derived neurotrophic factor mediated by an adeno-associated virus vector in a transgenic animal model of amyotrophic lateral sclerosis. *J Neurosci*, **22**: 6920-6928.

Xiao, W., Chirmule, N., Berta, S.C., Mccullough, B., Gao, G. and Wilson, J.M. (1999). Gene therapy vectors based on adeno-associated virus type 1. *J Virol*, **73**: 3994-4003.

Yang, Y., Hentati, A., Deng, H.X., Dabbagh, O., Sasaki, T., Hirano, M., Hung, W.Y., Ouahchi, K., Yan, J., Azim, A.C., Cole, N., Gascon, G., Yagmour, A., Ben-Hamida, M., Pericak-Vance, M., Hentati, F., and Siddique, T. (2001). The gene encoding alsin, a protein with three guanine-nucleotide exchange factor domains, is mutated in a form of recessive amyotrophic lateral sclerosis. *Nat Genet*, **29**: 160-165.

Zhong, X.H., Haycock, J.W., Shannak, K., Robitaille, Y., Fratkin, J., Koeppen, A.H., Hornykiewicz, O., and Kish, S.J. (1995). Striatal dihydroxyphenylalanine decarboxylase and tyrosine hydroxylase protein in idiopathic Parkinson's disease and dominantly inherited olivopontocerebellar atrophy. *Mov Disord*, **10**: 10-17.

Zolotukhin, S., Potter, M., Zolotukhin, I., Sakai, Y., Loiler, S., Fraites, T.J., Chiodo, V.A., Phillipsberg, T., Muzyczka, N., Hauswirth, W.W., Flotte, T.R., Byrne, B.J. and Snyder, R.O. (2002). Production and purification of serotype 1, 2, and 5 recombinant adeno-associated viralvectors. *Methods*, **28**: 158_167.

6. SUMMARY — The recombinant adeno-associated viral (rAAV) vector is a suitable vehicle for delivering therapeutic genes into mammalian central nervous system and muscle. Long-term expression of transgene is achieved without remarkable toxicity and inflammation. Using rAAV vectors, we attempted to restore motor functions in animal models of Parkinson's disease (PD) and amyotrophic lateral sclerosis (ALS). To achieve efficient production of dopamine (DA) in the striatum, we made rAAV vectors expressing DA-synthesizing enzymes: tyrosine hydroxylase, aromatic L-amino acid decarboxylase, and GTP cyclohydrolase I. Stereotaxic injection of these vectors into the unilateral putamen of a primate model of PD resulted in amelioration of motor dysfunctions with robust transgene expression in the treated putamen. An alterative strategy for gene therapy in PD is rAAV vector-mediated gene transfer of a glial cell line-derived neurotrophic factor (GDNF) gene into the striatum. Sustained expression of GDNF rescued nigral neurons and led to functional recovery in a rat model of PD. Protective effects on spinal motoneurons were also achieved by gene transfer of GDNF into muscles in transgenic ALS mice. Gene therapy using rAAV vectors may offer novel and feasible treatment options in neurodegenerative disease.

Key words: adeno-associated virus; Parkinson's disease; amyotrophic lateral sclerosis.

ARTHRITIS & RHEUMATISM
Vol. 52, No. 1, January 2005, pp 164–170
DOI 10.1002/art.20739

Repair of Articular Cartilage Defect by Autologous Transplantation of Basic Fibroblast Growth Factor Gene–Transduced Chondrocytes With Adeno-Associated Virus Vector

Naoki Yokoo,[1] Tomoyuki Saito,[1] Masaaki Uesugi,[1] Naomi Kobayashi,[1] Ke-Qin Xin,[1] Kenji Okuda,[1] Hiroaki Mizukami,[2] Keiya Ozawa,[2] and Tomihisa Koshino[1]

Objective. **To examine the effects of basic fibroblast growth factor (bFGF) gene–transduced chondrocytes on the repair of articular cartilage defects.**

Methods. **LacZ gene or bFGF gene was transduced into primary isolated rabbit chondrocytes with the use of a recombinant adeno-associated virus (AAV) vector. These gene-transduced chondrocytes were embedded in collagen gel and transplanted into a full-thickness defect in the articular cartilage of the patellar groove of a rabbit. The efficiency of gene transduction was assessed according to the percentage of LacZ-positive cells among the total number of living cells. The concentration of bFGF in the culture supernatant was measured by enzyme-linked immunosorbent assay to confirm the production by bFGF gene–transduced chondrocytes. At 4, 8, and 12 weeks after transplantation, cartilage repair was evaluated histologically and graded semiquantitatively using a histologic scoring system ranging from 0 (complete regeneration) to 14 (no regeneration) points.**

Results. **LacZ gene expression by chondrocytes was maintained until 8 weeks in >85% of the in vitro population. LacZ-positive cells were found at the transplant sites for at least 4 weeks after surgery. The mean concentration of bFGF was significantly increased in bFGF gene–transduced cells compared with control cells ($P < 0.01$). Semiquantitative histologic scoring indicated that the total score was significantly lower in the bFGF-transduced group than in the control group throughout the observation period.**

Conclusion. **These results demonstrated that gene transfer to chondrocytes by an ex vivo method was established with the AAV vector, and transplantation of bFGF gene–transduced chondrocytes had a clear beneficial effect on the repair of rabbit articular cartilage defects.**

Damage of articular cartilage leads to joint dysfunction associated with pain or limited range of motion and usually progresses to degeneration of the articular surface, resulting in osteoarthritis. It is well recognized that articular cartilage is a highly differentiated tissue with a limited capacity for self-repair. Current therapy for osteoarthritis consists of short-acting antiinflammatory drugs, intraarticular injection of steroids or other agents, such as hyaluronic acid, and surgical intervention. However, these treatments may not relieve joint pain completely. Therefore, cartilage repair seems to be essential for the prevention of a catastrophic outcome in a joint. Several studies describing the successful repair of osteochondral defects by the transplantation of cultured chondrocytes have been reported (1). However, a major problem with cartilage repair by autologous chondrocyte transplantation is that a large quantity of chondrocytes from normal articular cartilage is required, whereas donor sites have a limited capacity to provide chondrocytes.

Supported by a grant-in-aid for Scientific Research and by the Yokohama Foundation for the Advancement of Medical Science.

[1]Naoki Yokoo, MD, Tomoyuki Saito, MD, PhD, Masaaki Uesugi, MD, PhD, Naomi Kobayashi, MD, Ke-Qin Xin, MD, PhD, Kenji Okuda, MD, PhD, Tomihisa Koshino, MD, PhD: Yokohama City University School of Medicine, Yokohama, Japan; [2]Hiroaki Mizukami, MD, PhD, Keiya Ozawa, MD, PhD: Jichi Medical School, Tochigi, Japan.

Address correspondence and reprint requests to Naoki Yokoo, MD, Department of Orthopaedic Surgery, Yokohama City University School of Medicine, 3-9 Fukuura, Kanazawa-ku, Yokohama 236-0004, Japan. E-mail: Napoleon@nyc.odn.ne.jp.

Submitted for publication February 4, 2004; accepted in revised form September 27, 2004.

Many studies have demonstrated that basic fibroblast growth factor (bFGF) is one of the most potent of the various growth factors for cartilage repair (2–6). In order to establish an efficient approach for the treatment of cartilage defects, it may be advantageous to maintain a certain level of growth factor locally for a long time.

A new therapeutic approach to cartilage repair, gene therapy, has been described, in which genes are transduced into chondrocytes with the use of naked DNA or viral vectors (7–10). However, problems with this method are related to the ability to obtain high-efficiency transduction, to maintain long-term expression of the therapeutic gene, and safety. Recently, the adeno-associated virus (AAV) has been recognized as a tool for transducing a gene into target cells (11–14). Gene therapy with AAV has several advantages, including the lack of virulence of the wild-type virus, the safety, since there is no replication activity alone, the ability to transduce to nondividing cells, the integration into the host genome, and the long-term expression of the transduced gene.

In this study, we attempted to use this new delivery vector to repair cartilage defects, in an ex vivo method. The purpose of this study was to evaluate the utility of the AAV vector for ex vivo gene delivery to chondrocytes and to investigate the repair of an articular cartilage defect by transplantation of bFGF gene–transduced chondrocytes.

MATERIALS AND METHODS

AAV vector production. Two AAV constructs were prepared for this study: AAV-LacZ contained the bacterial β-galactosidase (LacZ) gene and AAV-bFGF contained the bFGF gene, which harbors a nuclear localization signal under the regulation of the cytomegalovirus immediate early promoter. The AAV subtype 2 vector plasmid used in this study, pLacZ, was derived from the vector plasmid pW1, which contains the LacZ gene, as previously described (15). Recombinant bFGF gene (GenBank accession no. X07285) was obtained from Takeda Chemical Industries (Osaka, Japan). A fragment containing bFGF complementary DNA was amplified by polymerase chain reaction using the following primer pairs with the *Eco* RI or the *Xho* I site: 5′-ATGAATTCATGGCTGCCGGCAGCATCACTTCGCTT-3′ and 5′-ATCTCGAGAGAGTCAGCTCTTAGCAGAC-3′. The fragment was subcloned between the *Eco* RI and *Xho* I sites of the pLacZ AAV vector plasmid to replace the LacZ gene (pbFGF). An AAV helper plasmid containing subtype 2 AAV *rep* and *cap* genes, which are required for replication and capsid formation of AAV vectors, pIM45 was used. A plasmid containing the E2A, E4, and VA genes of the adenovirus genome, pladeno-1, was used in place of helper adenovirus for AAV vector production.

Subconfluent human fetal kidney cells (293 cells) were cotransfected by the calcium phosphate coprecipitation method with pbFGF, pIM45, and pladeno-1 to produce the AAV-inducing bFGF gene (AAV-bFGF). After 48 hours, the cells were harvested and lysed in Tris HCl buffer (10 m*M* Tris HCl, 150 m*M* NaCl, pH 8.0) through 3 cycles of freezing and thawing. One round of sucrose precipitation and 2 rounds of CsCl density-gradient ultracentrifugation were performed to isolate AAV-bFGF from the lysates. The vector titer was determined by quantitative DNA dot-blot hybridization of the DNase I–resistant fraction.

Isolation of chondrocytes. Thirty-nine 10-week-old Japanese white rabbits (Oriental Yeast Company, Tokyo, Japan), weighing an average of 1.8 kg, were used in this study. They were divided into 3 groups: 9 for the LacZ-transduced group, 12 for the bFGF-transduced group, and 18 for the control group. Under intravenous anesthesia with pentobarbital sodium (Somnopentyl; Schering-Plough, Union, NJ), articular cartilage tissues (4 × 4–mm slices) were harvested from the patellar groove of the right knee, washed 3 times in phosphate buffered saline (PBS), and cut into small pieces. The pieces were treated with 0.05% trypsin and 0.001*M* EDTA (Gibco BRL, Gaithersburg, MD) for 30 minutes at 37°C and digested sequentially with 0.25% collagenase (type II collagenase; Worthington, Lakewood, NJ) for 3 hours at 37°C. The isolated chondrocytes were washed 3 times with PBS.

The mean number of cells collected from each rabbit was 2.4×10^5 (SD 0.5×10^5). These cells were divided into 4–6 culture wells and cultured in 24-well flat-bottomed plates (Falcon, Lincoln Park, NJ) at a concentration of 5×10^4 cells/well in 0.5 ml of Dulbecco's modified Eagle's medium (DMEM; Sigma, St. Louis, MO) supplemented with 10% fetal calf serum (FCS) and antibiotics (100 units/ml of penicillin G, 0.1 mg/ml of streptomycin; Gibco BRL) (DMEM–FCS), at 37°C in an atmosphere of 5% CO_2 in air.

Gene transduction into chondrocytes. Chondrocytes were cultured for 3 days, removed from the growth medium, and washed once with serum-free medium. To the culture wells for the transduced group was added 500 μl of serum-free DMEM containing AAV-LacZ or AAV-bFGF to enable quantification of transgene expression at the optimal number of viral particles (10^5 particles per cell) determined from the LacZ gene group experiments. To culture wells for the control group was added 500 μl of serum-free DMEM containing Tris buffer alone. After incubation for 1 hour at 37°C, 500 μl of DMEM–FCS was added to each culture well for both culture groups. One sample from each rabbit was used for autologous transplantation. The remaining samples were used for in vitro experiments.

Twenty samples from the LacZ-transduced group and 20 from the control group were used for the experiment to determine the efficacy of gene transduction in vitro. Culture medium was exchanged twice a week after gene transduction up to the time of analysis. At 3, 7, 14, 28, and 56 days after transduction, LacZ expression was assessed using the X-Gal staining technique (16), as follows. Cells were washed 3 times with PBS and fixed with 0.5% glutaraldehyde for 10 minutes, followed by 2 rinses in PBS containing 1 mmole/liter of $MgCl_2$. The cells were finally incubated with X-Gal substrate (1 mg/ml of X-Gal, 1 mmole/liter of $MgCl_2$, 5 mmoles/liter of $K_4Fe[CN]_6/K_3Fe[CN]_6$ in PBS) for 12 hours at 37°C. Efficiency of gene transduction was calculated as the average percentage

of X-Gal–positive cells per total number of living cells in 3 randomly selected fields viewed with an optical microscope.

Measurement of bFGF concentration in culture medium. Samples from 12 rabbits in the bFGF-transduced group and from 12 rabbits in the control group were used for determinations of accumulated bFGF production in the culture supernatant. The culture medium was not changed at each sampling of either group. At 3, 7, and 14 days after transduction, culture supernatants were collected from every 4 bFGF-transduced or control group culture wells, respectively, and after centrifugation, were stored at –80°C until analyzed. The bFGF concentration in the culture supernatants was measured by enzyme-linked immunosorbent assay (ELISA) using a bFGF-specific ELISA kit (Quantikine; R&D Systems, Minneapolis, MN) according to the manufacturer's instructions.

Autologous transplantation of gene-transduced chondrocytes into an articular cartilage defect. Chondrocytes from the LacZ-transduced, bFGF-transduced, and control groups were cultured for 1 week after gene transduction, collected from the culture wells by trypsinization, and then centrifuged. The supernatant was removed, and chondrocytes were embedded in a 0.2% solution of type I collagen (Cellgen; Koken, Tokyo, Japan) at a density of 1×10^6/ml. For autologous transplantation, chondrocytes were suspended in the collagen gel by incubation at 37°C for 1 hour.

Rabbits were anesthetized with pentobarbital sodium, and the left hind leg of each rabbit was sterilized for surgery. A 3-cm medial parapatellar incision was made over the knee, and the patella was dislocated laterally. A full-thickness defect in the articular cartilage (5 mm in diameter; 3 mm deep) was made in the patellar groove using a hand drill. The collagen gel containing $\sim 7.5 \times 10^4$ autologous chondrocytes was transplanted into the full-thickness defect. A periosteal flap of $\sim 5 \times 5$ mm was harvested from the anteromedial surface of the tibia and sutured to the peripheral rim of the artificial defect with 5-0 nylon thread. The cambium layer of the periosteal flap was faced toward the joint space. The rabbits were allowed to move freely immediately after surgery.

Among the 39 rabbits, LacZ-transduced chondrocytes were transplanted into 9, bFGF-transduced chondrocytes into 12, and chondrocytes without gene transduction into the remaining 18.

Evaluation of LacZ expression at the site of transplantation. Rabbits from the LacZ-transduced (n = 3) and control (n = 2) groups were killed at 1, 2, and 4 weeks after transplantation. The specimens were harvested from the patellar groove, embedded in TissueTek OCT compound (Sakura Finetek USA, Torrance, CA), and immediately frozen in nitrogen liquid. The frozen specimens were sectioned into 20-μm slices with a cryotome (Coldtome CM-502; Sakura Seiki, Tokyo, Japan) and double-stained with X-Gal and hematoxylin and eosin (H&E).

Histologic evaluation of repair cartilage. Rabbits from the bFGF-transduced (n = 4) and control (n = 4) groups were killed at 4, 8, and 12 weeks after transplantation. The distal part of the femur was resected en bloc, fixed with 10% buffered formalin, and decalcified with a 0.5*M* EDTA solution. Sagittal sections were prepared and stained with H&E, toluidine blue, or Safranin O–fast green. The histologic features of each specimen were evaluated semiquantitatively using the histologic scoring system described by Wakitani et al (17). This system consists of 5 categories (cell morphology, matrix staining, surface regularity, cartilage thickness, and integration of donor with host) scored on a 0–14-point scale, where 0 = complete regeneration and 14 = no regeneration.

Statistical analysis. Data are expressed as the mean ± SD. The statistical significance of differences was calculated with the use of StatView software (version J-5.0; Abacus Concepts, Berkeley, CA). One-way analysis of variance and the Mann-Whitney U test were used for analyzing statistical significance. *P* values less than 0.05 were considered significant.

RESULTS

In vitro experiment. *Efficiency of gene transduction of chondrocytes.* The efficiency of gene transduction was determined for chondrocytes transfected with AAV-LacZ at 7 days after transduction. The mean ± SD percentage of LacZ-positive cells among the total number of living cells was 43.7 ± 8.8%, 62.4 ± 5.1%, 97.7 ± 0.6%, and 98.2 ± 1.5% at a vector dose of 10^3, 10^4, 10^5, and 10^6 particles/cell, respectively (Figure 1). The percentage of successfully transduced chondrocytes increased in a vector dose–dependent manner. A vector dose of $>10^6$ particles/cell did not improve the transduction rate. The optimal dose of virus that was required to achieve transduction of ~100% of the chondrocytes was determined to be 10^5 particles/cell.

LacZ gene expression was highly maintained until 56 days after gene transduction. The mean ± SD percentage of LacZ-positive cells was 69.4 ± 15.1%, 97.7 ± 0.6%, 97.2 ± 1.8%, 95.8 ± 2.9%, and 85.8 ± 6.2% at 3, 7, 14, 28, and 56 days after transduction, respectively (Figure 2). The greatest population of

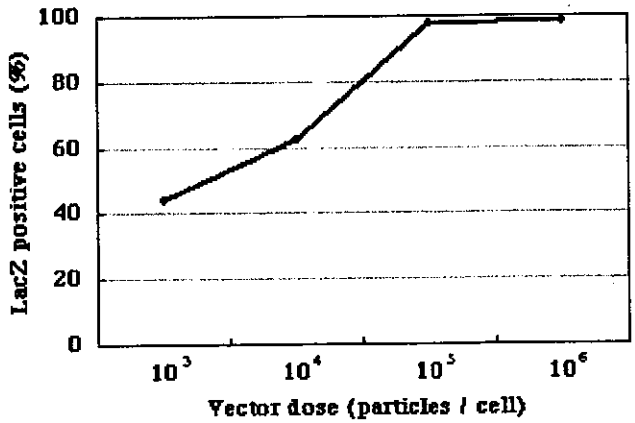

Figure 1. Vector dose–dependent LacZ expression in cultured chondrocytes. On day 7 after adeno-associated virus–LacZ transduction into chondrocytes, LacZ expression was assessed by X-Gal staining. The percentages of LacZ-positive cells among the total number of living cells were 43.7%, 62.4%, 97.7%, and 98.2% at doses of 10^3, 10^4, 10^5, and 10^6 particles/cell, respectively.

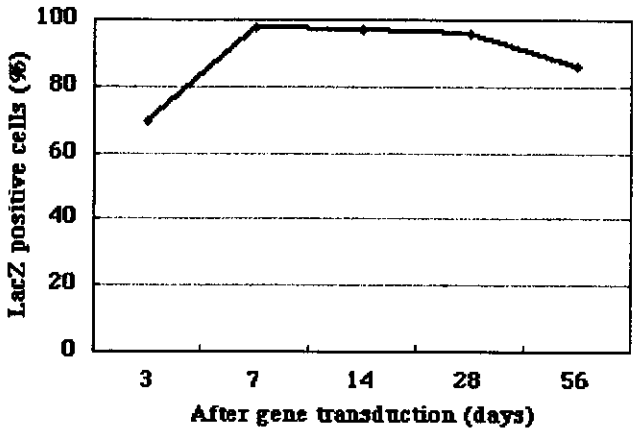

Figure 2. Time-dependent expression of LacZ in cultured chondrocytes. The percentages of LacZ-positive cells were 69.4%, 97.7%, 97.2%, 95.8%, and 85.8% at 3, 7, 14, 28, and 56 days after transduction, respectively.

LacZ-expressing cells was 97.7% at 7 days (Figure 3A), and more than 85% of the population was maintained up to 56 days. Cells without LacZ transduction in the control group failed to reveal LacZ expression at any sampling point (Figure 3B). There was no microscopic evidence of cell death or cytopathologic changes in the transduced cells as determined by optical microscopy.

Expression of bFGF gene by transduced chondrocytes. Production of bFGF was detected in both bFGF-transduced cells and control cells. The mean ± SD bFGF concentration in culture supernatants from the bFGF-transduced cells was 88.2 ± 9.8 ng/ml, 130.9 ± 28.8 ng/ml, and 240.6 ± 22.5 ng/ml at 3, 7, and 14 days after transduction, respectively (Figure 4). In control

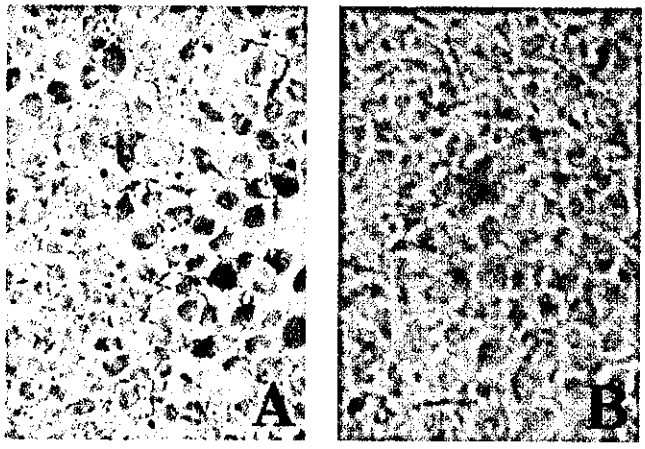

Figure 3. Photomicrographs of transduced chondrocytes stained with X-Gal. **A,** LacZ group chondrocytes were stained with X-Gal on day 7 after adeno-associated virus–LacZ transduction. LacZ-positive cells are stained blue. **B,** Control group chondrocytes showed no LacZ-positive cells. (Original magnification × 100.)

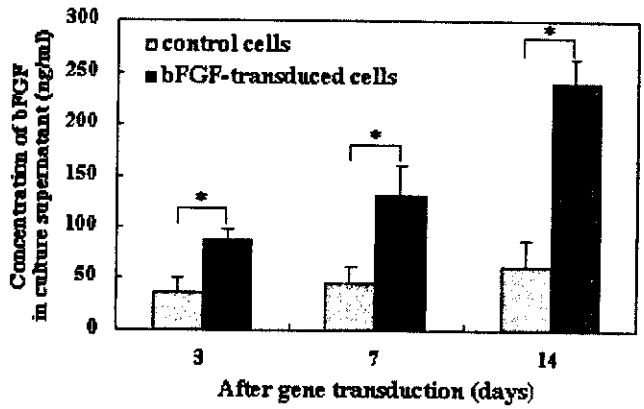

Figure 4. Concentration of basic fibroblast growth factor (bFGF) in culture supernatants of bFGF-transduced chondrocytes. Culture supernatants of control and bFGF-transduced cells were collected on days 3, 7, and 14 after transduction, and the bFGF concentration was determined by enzyme-linked immunosorbent assay. Transduction of the bFGF gene significantly elevated the secretion of bFGF (* = $P <$ 0.01).

cells, the bFGF concentration was 35.0 ± 15.8 ng/ml, 44.5 ± 16.4 ng/ml, and 62.3 ± 25.8 ng/ml at 3, 7, and 14 days after transduction, respectively. The bFGF concentration was significantly greater in bFGF-transduced cells than in the control cells on all sampling days ($P <$ 0.01).

The mean number of chondrocytes in the bFGF-transduced group was 14.1×10^4 (SD 1.1×10^4) and 34.8×10^4 (SD 6.2×10^4) at 7 and 14 days after transduction, respectively. In the control group, the numbers were 6.4×10^4 (SD 1.5×10^4) and 17.0×10^4 (SD 3.2×10^4) at 7 and 14 days after transduction, respectively. The mean number of chondrocytes in the bFGF-transduced group was significantly higher than that in the control group during the period of culture ($P < 0.01$).

In vivo experiment. *LacZ expression at the transplant site.* Throughout the observation period, X-Gal staining of LacZ-transduced cells showed cells with blue nuclei distributed across the entire regenerated cartilage under the layer covered by the transplanted periosteal flap. The controls, which received transplants without LacZ-transduced chondrocytes, did not show LacZ-positive cells at any week of sampling. No adverse effects related to the virus were observed in this ex vivo gene transfer experiment.

Macroscopic findings at the site of transplantation of the bFGF-transduced chondrocytes. Macroscopic observation of the transplant site showed regeneration of the articular cartilage defect in both the bFGF-transduced and control groups. At 12 weeks, the margin between the regenerated tissue and the

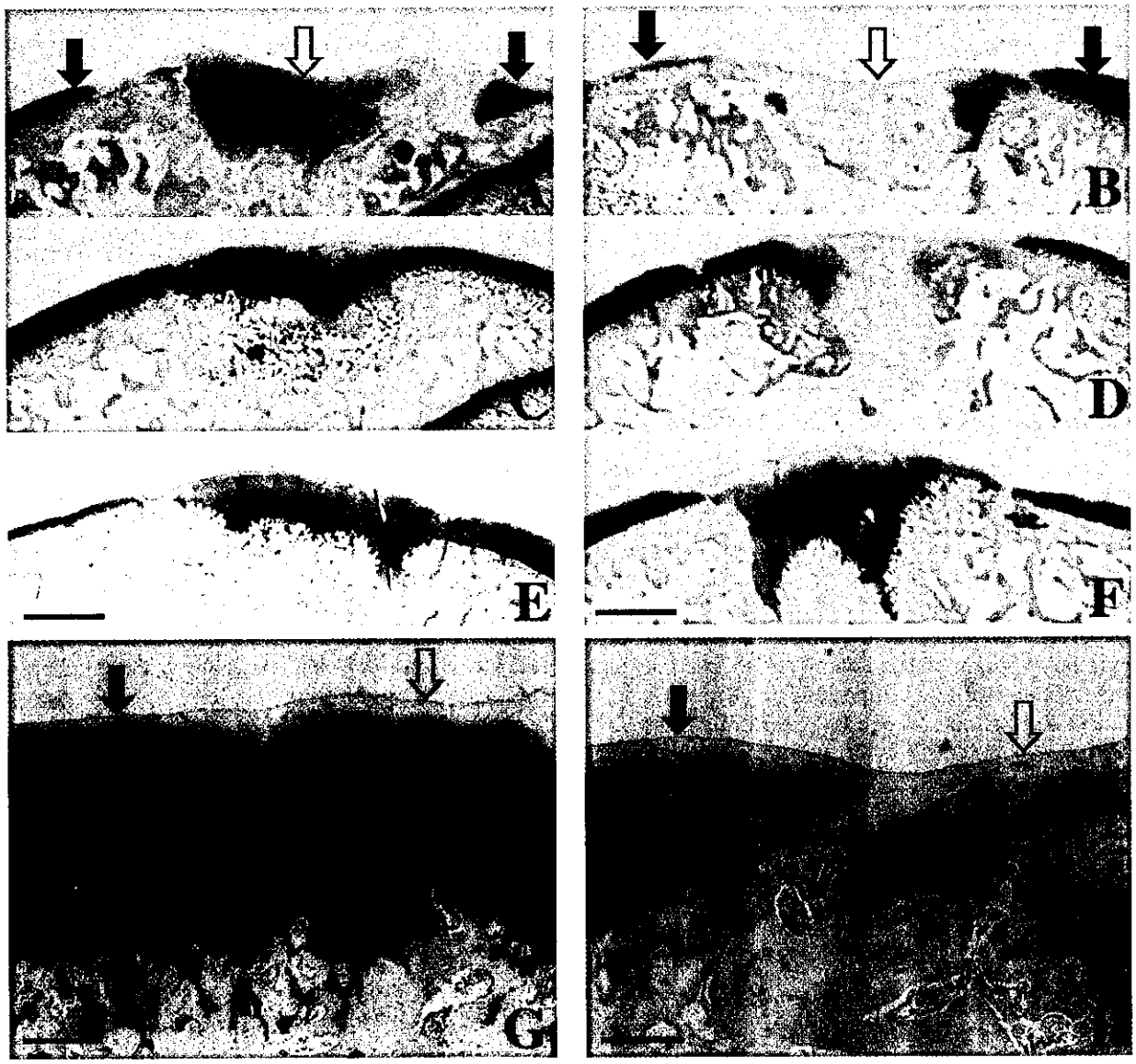

Figure 5. Photomicrographs of sagittal sections of articular cartilage defects in rabbits after transplantation with basic fibroblast growth factor (bFGF)–transduced chondrocytes (**A, C, E,** and **G**) and control chondrocytes (**B, D, F,** and **H**). Photomicrographs of the junction area are also shown (**G** and **F**). In the bFGF-transduced group, at 4 weeks (**A**), the deep layer is composed of round chondrocytes, but the matrix is weakly stained. At 8 weeks (**C**), the matrix is more distinctly stained, but the superficial region is weakly stained. At 12 weeks (**E** and **G**), the matrix is intensely metachromatically stained, and there is reconstitution of the osteochondral junction in most specimens. In the control group, at 4 weeks (**B**) and 8 weeks (**D**), the matrix is faintly stained. At 12 weeks (**F** and **H**), the deep layer of the matrix stained well, but staining is reduced in the superficial layers. **Solid arrows** indicate regenerated cartilage; **open arrows** indicate surrounding normal cartilage. Sections were stained with Safranin O–fast green. Bars in **A** and **F** = 1 mm; bars in **G** and **H** = 100 μm.

original cartilage was not distinguishable in both groups. The surface of the regenerated cartilage closely resembled normal cartilage in the bFGF-transduced group, but that in the control group could still be distinguished from surrounding normal cartilage. No sign of osteoarthrosis, such as erosion of cartilage or osteophyte formation, was seen in any of the knees during the observation period.

Histologic findings of regenerated cartilage following transplantation of bFGF-transduced chondrocytes. At 4 weeks after transplantation, in the tissues obtained from the bFGF-transduced group, the deep part of the

Table 1. Histologic scores of regenerated cartilage at 4, 8, and 12 weeks*

Weeks after transplantation	Control group	bFGF-transduced group
4	8.8 ± 1.0	6.5 ± 0.6†
8	7.0 ± 1.4	4.3 ± 1.0†
12	5.5 ± 1.7	2.8 ± 1.0†

* The histologic features were scored on a 0–14-point scale as described by Wakitani et al (17), where 0 represents complete regeneration and 14 represents no regeneration. Values are the mean ± SD. bFGF = basic fibroblast growth factor.
† $P < 0.01$ versus controls.

regenerated tissue was composed of round chondrocytes, with an extracellular matrix that stained weakly with Safranin O (Figure 5A). There was no integration of the edges of the regenerated tissue with the adjacent normal cartilage or reconstitution of the osteochondral junction in any specimen. In the control group, the extracellular matrix was faintly stained with Safranin O (Figure 5B).

At 8 weeks, the bFGF-transduced group showed an extracellular matrix that was more distinctly stained with Safranin O in the deep part, while the superficial part was weakly stained (Figure 5C). Although both edges were integrated with the adjacent normal cartilage, reconstitution of the osteochondral junction was not seen in any specimen. The tissues from the control group at 8 weeks were essentially the same as those at 4 weeks (Figure 5D).

In the bFGF-transduced group at 12 weeks, the intensity and thickness of the extracellular matrix that was metachromatically stained with Safranin O were increased as compared with the findings at 4 and 8 weeks, and the microstructure of the regenerated tissue resembled the surrounding normal cartilage (Figures 5E and G). There was reconstitution of the osteochondral junction in most of the specimens. In the control group, the deep layer of the regenerated cartilage matrix stained well with Safranin O, but staining was reduced in the superficial layers (Figures 5F and H). There was no reconstitution of the osteochondral junction in any of the control specimens.

The Wakitani score was 6.5 ± 0.6, 4.3 ± 1.0, and 2.8 ± 1.0 points (mean ± SD) at 4, 8, and 12 weeks after transplantation, respectively, in the bFGF-transduced group. In the control group, the score was 8.8 ± 1.0, 7.0 ± 1.4, and 5.5 ± 1.7 points at 4, 8, and 12 weeks after transplantation, respectively (Table 1). The scores in both groups gradually decreased throughout the experimental period. However, the score in the bFGF-transduced group became significantly lower than that in the control group with the passage of time postoperatively ($P < 0.01$).

DISCUSSION

Autologous chondrocyte transplantation has been successfully applied in recent years to the treatment of focal cartilage defects in a series of patients (18). Autologous chondrocytes for grafting are harvested from non–weight-bearing areas, cultured in vitro, reinjected into the cartilage defect, and the area is covered with a periosteal flap that is sutured in place. However, this method may be limited to small local cartilage defects, since the number of cells collected from donor sites to be used for cultivation is still limited.

Augmentation of the procedure with bFGF for help in repairing the cartilage has been reported to be efficacious (4–6,19). Weisser et al (4) reported that among several different growth factors used to treat transplanted chondrocytes, positive effects on cartilage repair were observed only with the bFGF-treated chondrocyte implants (4). Previous studies showed that exogenous bFGF induces the proliferation of chondrocytes, the maturation of cartilage, and the differentiation of mesenchymal cells, and it stimulates the synthesis of cartilaginous matrix (5,6). Otsuka et al (19) reported that continuous administration of bFGF using an osmotic pump had a clearly beneficial effect on repair of cartilage defects. However, bFGF alone did not lead to complete structural restitution of hyaline cartilage to repair the full-thickness defects of articular cartilage. Prolonged local expression of bFGF by transduction of the genetic code of bFGF into chondrocytes would be an efficient treatment for articular cartilage defects.

For the repair of cartilage defects with gene therapy, it may be necessary to obtain high-efficiency transduction and continuous local expression of the therapeutic gene. Several studies have demonstrated that the AAV vector has the ability to highly efficiently transduce a gene into cells, to integrate into the host genome, and to express the transduced gene for a long time (20–22). There are studies of the utility of the AAV vector for joint disease that demonstrated high-efficiency gene delivery to the synovium in vivo (23) or gene transduction to cultured chondrocytes in vitro (24). Delivering genes directly to the surface of the abnormal articular cartilage in order to accelerate cartilage repair could result in a long-term treatment. The advantage of ex vivo gene delivery would be direct delivery of the therapeutic gene to the abnormal articular cartilage and the ability to limit the area of gene expression to the cartilage defect alone. In our previous study, ex vivo

gene transfer to periosteum-derived cells using an AAV vector induced LacZ expression for 4 weeks in vivo (25).

In this study, high-efficiency LacZ gene transduction into chondrocytes was obtained long-term in vitro, and LacZ gene expression in vivo was sustained without any adverse effects. These findings suggest that gene transfer to an articular cartilage defect by use of the ex vivo method was established with the AAV vector. Cartilage repair was slightly inferior to that described in previous reports, even though we used 10-week-old rabbits for the experiment. One of the reasons was thought to be differentiation to fibrous chondrocytes during the 1-week culture before transplantation. The cell number and the bFGF secretion were significantly increased in bFGF-transduced chondrocytes compared with the control chondrocytes in vitro. Furthermore, the histologic appearance of the transplant site in the bFGF-transduced group was fully repaired compared with that in the control group. The repair at a comparatively early stage was apparently different between bFGF-transduced and null chondrocytes even at 12 weeks. Continuous bFGF secretion by gene transfer seemed to be an effective way to promote cartilage repair.

These results demonstrate that repair of full-thickness defects in rabbit articular cartilage can be enhanced by transplantation of bFGF gene–transduced chondrocytes. This method seems to be one of the best techniques for achieving repair of articular cartilage defects.

ACKNOWLEDGMENT

We thank Avigen, Inc. (Alameda, CA) for supplying the plasmid for the production of the AAV vector.

REFERENCES

1. Brittberg M, Lindahl A, Nilsson A, Ohlsson C, Isaksson O, Peterson L. Treatment of deep cartilage defects in the knee with autologous chondrocyte transplantation. N Engl J Med 1994;331: 889–95.
2. Kato Y, Gospodarowicz D. Sulfated proteoglycan synthesis by confluent cultures of rabbit costal chondrocytes grown in the presence of fibroblast growth factor. J Cell Biol 1985;100:477–85.
3. Hunziker EB, Rosenberg LC. Repair of partial-thickness defects in articular cartilage: cell recruitment from the synovial membrane. J Bone Joint Surg Am 1996;78:721–33.
4. Weisser J, Rahfoth B, Timmermann A, Aigner T, Brauer R, von der Mark K. Role of growth factors in rabbit articular cartilage repair by chondrocytes in agarose. Osteoarthritis Cartilage 2001; 9:48–54.
5. Shida J, Jingushi S, Izumi T, Iwaki A, Sugioka Y. Basic fibroblast growth factor stimulates articular cartilage enlargement in young rats in vivo. J Orthop Res 1996;14:265–72.
6. Cuevas P, Burgos J, Baird A. Basic fibroblast growth factor (FGF) promotes cartilage repair in vivo. Biochem Biophys Res Commun 1988;156:611–8.
7. Arai Y, Kubo T, Kobayashi K, Takeshita K, Takahashi K, Ikeda T, et al. Adenovirus vector-mediated gene transduction to chondrocytes: in vitro evaluation of therapeutic efficiency of transforming growth factor-β1 and heat shock protein 70 gene transduction. J Rheumatol 1997;24:1787–95.
8. Baragi VM, Renkiewicz RR, Qiu L, Brammer D, Riley JM, Sigler RE, et al. Transplantation of adenovirally transduced allogeneic chondrocytes into articular cartilage defects in vivo. Osteoarthritis Cartilage 1997;5:275–82.
9. Doherty PJ, Zhang H, Tremblay L, Manolopoulos V, Marshall KW. Resurfacing of articular cartilage explants with genetically-modified human chondrocytes in vitro. Osteoarthritis Cartilage 1998;6:153–9.
10. Kang BR, Marui T, Ghivizzani SC, Nita IM, Georgescu HI, Suh JK, et al. Ex vivo gene transfer to chondrocytes in full-thickness articular cartilage defects: a feasibility study. Osteoarthritis Cartilage 1997;5:139–43.
11. Schwarz EM. The adeno-associated virus vector for orthopaedic gene therapy [review]. Clin Orthop 2000;379 Suppl:S31–9.
12. Kaplitt MG, Leone P, Samulski RJ, Xiao X, Pfaff DW, O'Malley KL, et al. Long-term gene expression and phenotypic correction using adeno-associated virus vectors in the mammalian brain. Nat Genet 1994;8:148–54.
13. Xiao X, Li J, McCown TJ, Samulski RJ. Gene transfer by adeno-associated virus vectors into the central nervous system. Exp Neurol 1997;144:113–24.
14. Berns KI, Giraud C. Adenovirus and adeno-associated virus as vectors for gene therapy. Ann N Y Acad Sci 1995;772:95–104.
15. Xin KQ, Urabe M, Yang J, Nomiyama K, Mizukami H, Hamajima K, et al. A novel recombinant adeno-associated virus vaccine induces a long-term humoral immune response to HIV. Hum Gene Ther 2001;12:1047–61.
16. Price J, Turner D, Cepko C. Lineage analysis in the vertebrate nervous system by retrovirus-mediated gene transfer. Proc Natl Acad Sci U S A 1987;84:156–60.
17. Wakitani S, Goto T, Pineda SJ, Young RG, Mansour JM, Caplan AI, et al. Mesenchymal cell-based repair of large, full-thickness defects of articular cartilage. J Bone Joint Surg Am 1994;76: 579–92.
18. Richardson JB, Caterson B, Evans EH, Ashton BA, Roberts S. Repair of human articular cartilage after implantation of autologous chondrocytes. J Bone Joint Surg Br 1999;81:1064–8.
19. Otsuka Y, Mizuta H, Takagi K, Iyama K, Yoshitake Y, Nishikawa K. Requirement of fibroblast growth factor signaling for regeneration of epiphyseal morphology in rabbit full-thickness defects of articular cartilage. Dev Growth Differ 1997;39:143–56.
20. Kessler PD, Podsakoff GM, Chen X, McQuiston SA, Colosi PC, Matelis LA, et al. Gene delivery to skeletal muscle results in sustained expression and systemic delivery of a therapeutic protein. Proc Natl Acad Sci U S A 1996;93:14082–7.
21. Fisher KJ, Jooss K, Alston J, Yang Y, Haecker SE, High K, et al. Recombinant adeno-associated virus for muscle directed gene therapy. Nat Med 1997;3:306–12.
22. Herzog RW, Hastrom JN, Kung SH, Tai SJ, Wilson JM, Fisher KJ, et al. Stable gene transfer and expression of human blood coagulation factor IX after intramuscular injection of recombinant adeno-associated virus. Proc Natl Acad Sci U S A 1997;94:5804–9.
23. Goater J, Muller R, Kollias G, Firestein GS, Sanz I, O'Keefe RJ, et al. Empirical advantages of adeno associated viral vectors for in vivo gene therapy for arthritis. J Rheumatol 2000;27:983–9.
24. Arai Y, Kubo T, Fushiki S, Mazda O, Nakai H, Iwaki Y, et al. Gene delivery to human chondrocytes by an adeno associated virus vector. J Rheumatol 2000;27:979–82.
25. Kobayashi N, Koshino T, Uesugi M, Yokoo N, Xin KQ, Okuda K, et al. Gene marking in adeno-associated virus vector infected periosteum-derived cells for cartilage repair. J Rheumatol 2002; 29:2176–80.

Gene Therapy (2004) 11, 1772–1779

www.nature.com/gt

RESEARCH ARTICLE

Adeno-associated virus vector-mediated interleukin-10 gene transfer inhibits atherosclerosis in apolipoprotein E-deficient mice

T Yoshioka[1,2,3], T Okada[2], Y Maeda[1], U Ikeda[3], M Shimpo[1], T Nomoto[2], K Takeuchi[4], M Nonaka-Sarukawa[1], T Ito[1], M Takahashi[3], T Matsushita[2], H Mizukami[2], Y Hanazono[2], A Kume[2], S Ookawara[4], M Kawano[5], S Ishibashi[6], K Shimada[1] and K Ozawa[2]

[1]*Division of Cardiovascular Medicine, Jichi Medical School, Tochigi, Japan;* [2]*Division of Genetic Therapeutics, Center for Molecular Medicine, Jichi Medical School, Tochigi, Japan;* [3]*Department of Organ Regeneration, Shinshu University Graduate School of Medicine, Matsumoto, Japan;* [4]*Department of Anatomy, Jichi Medical School, Tochigi, Japan;* [5]*Department of Laboratory Medicine, Jichi Medical School, Tochigi, Japan; and* [6]*Division of Endocrine and Metabolism, Jichi Medical School, Tochigi, Japan*

Inflammation is a major contributor to atherosclerosis by its effects on arterial wall biology and lipoprotein metabolism. Interleukin-10 (IL-10) is an anti-inflammatory cytokine that may modulate the atherosclerotic disease process. We investigated the effects of adeno-associated virus (AAV) vector-mediated gene transfer of IL-10 on atherogenesis in apolipoprotein E (ApoE)-deficient mice. A murine myoblast cell line, C2C12, transduced with AAV encoding murine IL-10 (AAV2-mIL10) secreted substantial amounts of IL-10 into conditioned medium. The production of monocyte chemoattractant protein-1 (MCP-1) by the murine macrophage cell line, J774, was significantly inhibited by conditioned medium from AAV2-mIL10-transduced C2C12 cells. ApoE-deficient mice were injected with AAV5-mIL10 into their anterior tibial muscle at 8 weeks of age. The expression of MCP-1 in the vascular wall of the ascending aorta and serum MCP-1 concentration were decreased in AAV5-mIL10-transduced mice compared with AAV5-LacZ-transduced mice. Oil red-O staining of the ascending aorta revealed that IL-10 gene transfer resulted in a 31% reduction in plaque surface area. Serum cholesterol concentrations were also significantly reduced in AAV5-mIL10-transduced mice. To understand the cholesterol-lowering mechanism of IL-10, we measured the cellular cholesterol level in HepG2 cells, resulting in its significant decrease by the addition of IL-10 in a dose-dependent manner. Furthermore, IL-10 suppressed HMG-CoA reductase expression in the HepG2 cells. These observations suggest that intramuscular injection of AAV5-mIL10 into ApoE-deficient mice inhibits atherogenesis through anti-inflammatory and cholesterol-lowering effects.
Gene Therapy (2004) **11,** 1772–1779. doi:10.1038/sj.gt.3302348; Published online 21 October 2004

Keywords: *IL-10; AAV; atherosclerosis; cholesterol*

Introduction

The inflammatory reaction involves complex interactions between inflammatory cells (lymphocytes and macrophages) and vascular endothelial and smooth muscle cells. The disturbance of vascular wall integrity and homeostasis by inflammation is thought to be a major contributor to atherosclerosis. Therefore, an anti-inflammatory strategy may be a promising approach to prevent and treat atherosclerotic disease. Another critical feature of atherogenesis is lipid accumulation. Several large-scale clinical trials have demonstrated that lipid reduction therapy involving HMG-CoA reductase inhibitor (statin) is useful for atherosclerotic disorders, such as ischemic heart disease.[1,2] Recent studies have indicated that statins have pleiotropic effects on the atherogenic process, including an anti-inflammatory effect.[3] On the other hand, proinflammatory cytokines, such as tumor necrosis factor (TNF)-α, interleukin (IL)-1, and IL-6, have profound effects on lipid metabolism.[4] These findings suggest that there are complex interactions between inflammation and lipid metabolism.

IL-10, which is secreted by a wide variety of cells such as lymphocytes and macrophages, is a key inhibitor in a number of inflammatory responses,[5] including the production of proinflammatory cytokines and chemokines and the expression of endothelial adhesion molecules. IL-10 expression has been identified in early and advanced atherosclerotic plaques[6,7] and is thought to have potential antiatherogenic effects. Indeed, recent studies have shown that IL-10-transgenic mice fed a high-fat diet exhibit a decrease in atherogenesis.[8] Conversely, IL-10-deficient mice were found to suffer from more severe atherosclerosis, and the atherogenic tendency of these mice was ameliorated by the plasmid-mediated introduction of IL-10.[9] IL-10 is thought to have a protective role in human atherosclerotic disease as well.[10,11]

Despite the tremendous interest in the effects of cytokines on inflammation and lipoprotein metabolism, there have been few studies that have examined the

Correspondence: Dr K Ozawa, Division of Genetic Therapeutics, Center for Molecular Medicine, Jichi Medical School, 3311-1 Yakushiji, Minami-kawachi, Tochigi 329-0498, Japan
Received 9 November 2003; accepted 12 June 2004; published online 21 October 2004

influence of IL-10 on these processes *in vivo*.[12,13] As atherogenesis is a chronic process, the long-term expression of IL-10 is required in order to assess its effects on this disease. In this study, we have used adeno-associated virus (AAV) vectors for IL-10 gene transfer to investigate the antiatherosclerotic effects of IL-10 *in vivo*, because these vectors can transduce skeletal muscle and permit the sustained expression and systemic delivery of therapeutic proteins following a single intramuscular administration.[14]

Results

IL-10 expression in C2C12 cells

We first verified the integrity of our vectors *in vitro*. Differentiated C2C12 cells, murine myoblasts, were transduced with AAV encoding murine IL-10 (AAV2-mIL10) at various dosages and cultured for 48 h. The concentration of IL-10 in the conditioned medium was found to increase in a vector dose-dependent manner (Figure 1a). Western blot analysis demonstrated the presence of an 18-kDa product, the size expected for murine IL-10, in the conditioned medium of AAV2-mIL10-transduced C2C12 cells, but not in the conditioned medium of AAV2-LacZ-transduced cells (Figure 1b).

To evaluate the biological activity of secreted IL-10, we examined the influence of conditioned medium from AAV2-mIL10-transduced C2C12 cells on cytokine production by J774 cells, murine macrophages. As shown in Figure 1c, treatment with lipopolysaccharide (LPS) increased the production of the cytokines, IL-6, TNF-α, and monocyte chemoattractant protein-1 (MCP-1), from J774 cells. These increases were significantly inhibited by the addition of conditioned medium from AAV2-mIL10-transduced C2C12 cells, and the production of these cytokines was completely restored in the presence of anti-mIL-10 antibody (1 μg/ml). Unstimulated J774 cells did not exhibit any change in cytokine expression when exposed to the conditioned medium.

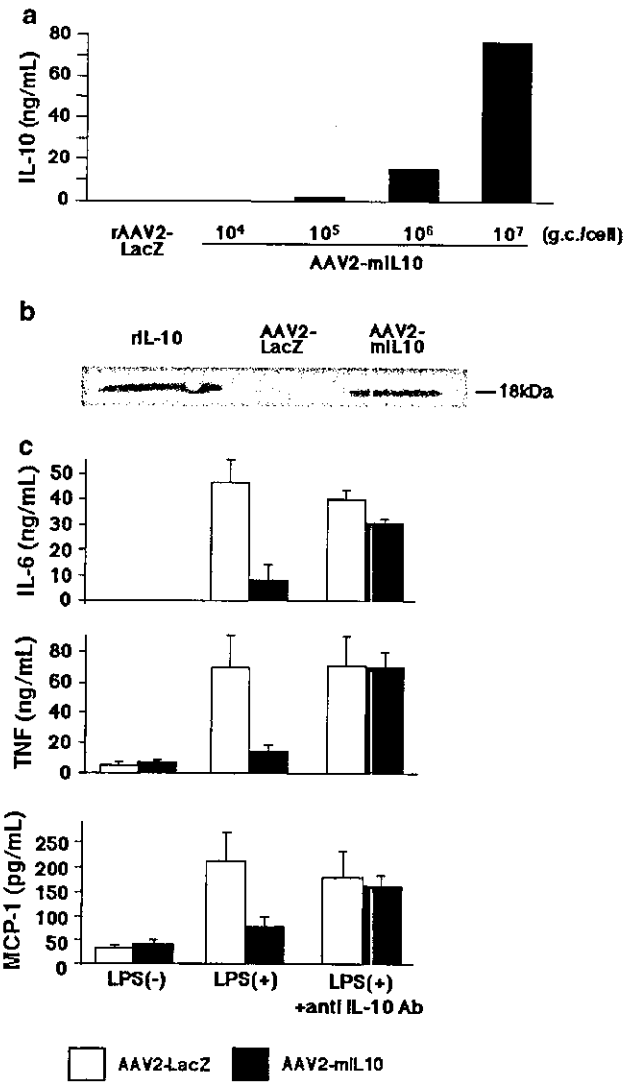

Figure 1 Transduction of the IL-10 gene into C2C12 cells with AAV2-mIL10. (a) Concentration of IL-10 in the conditioned medium of AAV2-mIL10-transduced C2C12 cells. The IL-10 concentration was measured by ELISA 48 h after transduction with the indicated number of genome copies per cell (g.c./cell). (b), Western blotting with an anti-IL-10 antibody was performed after immunoprecipitation of the conditioned medium of AAV2-mIL10- and AAV2-LacZ-transduced C2C12 cells. Recombinant mouse IL-10 (rIL-10) was used as a positive control. (c) LPS-stimulated J774 cells were incubated with the conditioned medium of AAV2-mIL10- (solid bars) or AAV2-LacZ (open bars)-transduced C2C12 cells for 24 h in the presence or absence of anti-IL-10 antibody (1 μg/ml). IL-6, TNF-α, and MCP-1 concentrations were analyzed by ELISA. Data are means ± s.e.m. (n = 4).

IL-10 expression in apolipoprotein E-deficient mice

We next injected AAV2-mIL10 and AAV5-mIL10 into the anterior tibial muscle of apolipoprotein E (ApoE)-deficient mice. The serum concentration of IL-10 increased in a vector dose-dependent manner, and the efficacy of transduction was higher in AAV5-mIL10-treated mice than in AAV2-mIL10-treated mice at the same vector dose (1×10^{13} genome copies/body) (Figure 2). When 1×10^{12} genome copies/body of AAV5-mIL10 were injected, the serum IL-10 levels (1.2–4.9 ng/ml) were maintained at a higher than physiological range (up to 160 pg/ml) for 8 weeks. Moreover, the serum IL-10 levels at 14 months were 398.3 ± 146.6 pg/ml.

Effect of IL-10 on MCP-1 expression

We then investigated the anti-inflammatory effects of IL-10 in ApoE-deficient mice by focusing on the expression of MCP-1, a potent chemokine implicated in atherogenesis. ApoE-deficient mice transduced with AAV5-mIL10 at 4 weeks old were evaluated at 8 weeks old. Few atherosclerotic lesions were detected by oil red-O staining at this time point. An immunohistochemical analysis of MCP-1 in the aortic sinus of ApoE-deficient mice revealed that MCP-1 expression was modestly suppressed in AAV5-mIL10-transduced mice, whereas it was clearly observed in the vascular wall of AAV5-LacZ-transduced mice (Figure 3a). Moreover, 8 weeks after gene transfer, the serum concentration of MCP-1 in AAV5-mIL10-transduced mice was significantly reduced compared with that in AAV5-LacZ-transduced mice (Figure 3b).

Effects of IL-10 on atherogenesis

We evaluated the lesion area in ApoE-deficient mice fed an atherogenic diet 8 weeks after gene transfer. As shown in Figure 4, the aortic sinus of mice transduced with AAV5-mIL10 revealed a significant decrease in oil

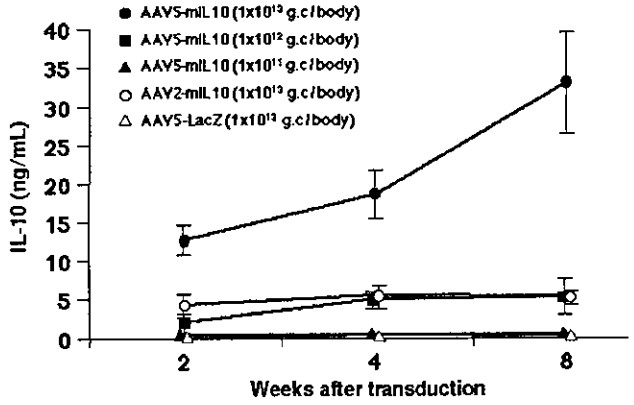

Figure 2 Serum concentration of IL-10 after transduction of AAV-mIL10 into the anterior tibial muscle of ApoE-deficient mice. ApoE-deficient mice at 8 weeks of age were inoculated with AAV2-mIL10 (1×10^{13} g.c./body), AAV5-mIL10 ($1 \times 10^{11} \sim 1 \times 10^{13}$ g.c./body), or AAV5-LacZ (1×10^{13} g.c./body) by injection into the anterior tibial muscle. At 2, 4, and 8 weeks after injection, the serum IL-10 concentration was measured. Data are means ± s.e.m. ($n = 3$–7).

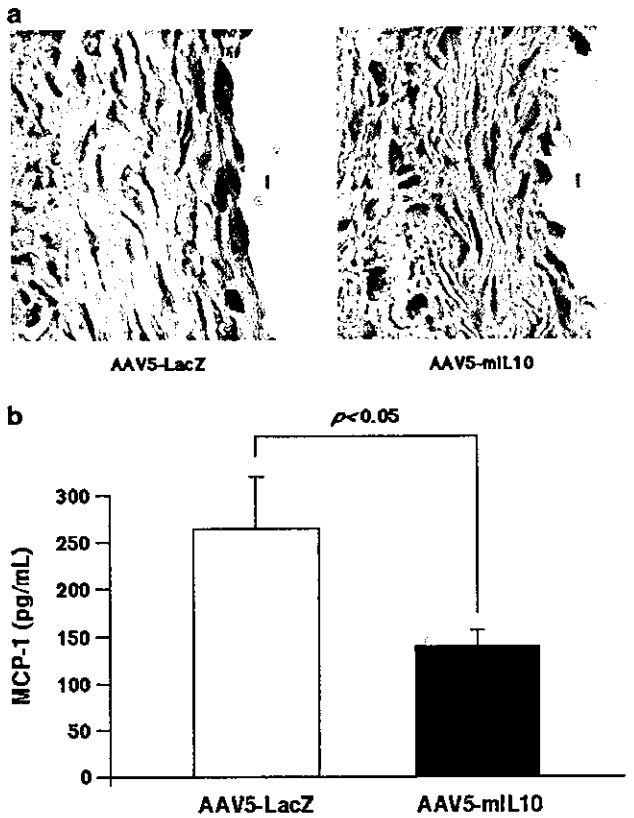

Figure 3 Systemic and local MCP-1 expression in ApoE-deficient mice. (a) Immunohistochemical staining of the aortic sinus segment in ApoE-deficient mice was performed 4 weeks after inoculation with AAV5-mIL10 (1×10^{12} g.c./body). Enhanced MCP-1 expression was observed in the vascular wall of AAV5-LacZ mice, but was suppressed in AAV5-mIL10-transduced mice. I, intima; A, adventitia. (b) The serum MCP-1 concentration in ApoE-deficient mice was measured 8 weeks after inoculation with AAV5-mIL10 or AAV5-LacZ. Means and s.e.m. for each group are presented as histograms ($n = 6$ for LacZ, $n = 13$ for IL-10).

red-O-positive areas compared to that of mice transduced with AAV5-LacZ. The systemic overexpression of IL-10 resulted in a 31% reduction in plaque surface area

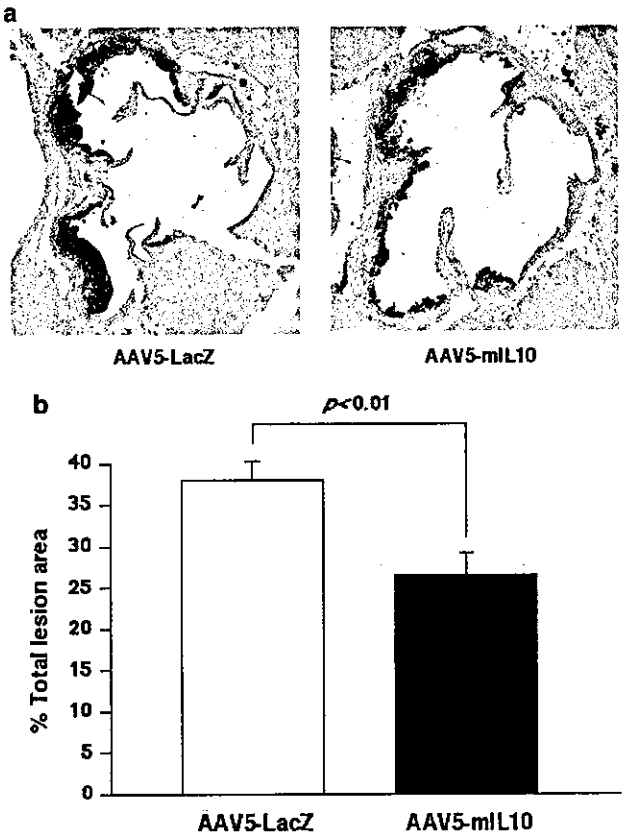

Figure 4 The inhibitory effect of IL-10 on atherogenesis in ApoE-deficient mice. (a) At 8 weeks after inoculation with AAV5-mIL10 (1×10^{12} g.c./body), the proximal aortas were removed, sectioned, and stained with oil red-O. (b) Oil red-O-positive areas were analyzed in comparison with the total cross-sectional vessel wall area. The average values for five sites from each animal were used for analysis. Means and s.e.m. for each group are presented as histograms ($n = 5$ for LacZ, $n = 9$ for IL-10).

(AAV5-IL-10, 26.5 ± 1.9% *versus* AAV5-LacZ, 37.7 ± 2.2% of total cross-sectional vessel wall area, $P < 0.01$). Figure 5 shows that serum MCP-1 concentration correlates with the extent of atherosclerotic lesion formation, suggesting that a decrease in MCP-1 expression is related to a decrease in atherosclerotic lesion formation.

Effect of IL-10 on lipids

We investigated the effects of IL-10 expression on the level of serum lipids. Total cholesterol levels were significantly reduced in the AAV5-mIL10-transduced mice (931 ± 432, 1074 ± 419 mg/dl) compared to the AAV5-LacZ-transduced mice (2212 ± 640, 1840 ± 421 mg/dl, 4 weeks and 8 weeks after gene transfer, respectively). Triglyceride level in the AAV5-IL10-transduced mice 8 weeks after gene transfer was also reduced (171.7 ± 67.3 mg/dl) compared to that in the AAV5-LacZ-transduced mice (291.6 ± 172.4 mg/dl, $P < 0.05$).

Nonlinear regression fitting to a sigmoidal dose curve revealed a high correlation between the serum cholesterol level and IL-10 concentration ($r = 0.857$), with an estimated EC_{50} of 5.3 ng/ml (Figure 6a). In addition, the serum cholesterol concentration positively correlated with the atherosclerotic lesion area ($r = 0.728$, $P < 0.01$; Figure 6b). IL-10 gene transfer did not affect body

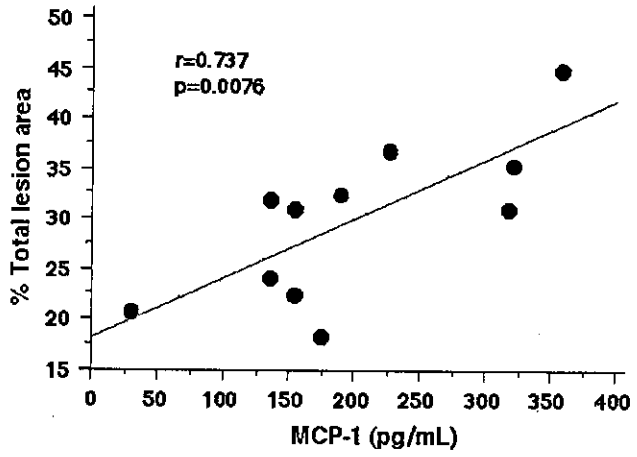

Figure 5 Correlation between serum MCP-1 concentration and extent of atherosclerotic lesion formation. The serum MCP-1 concentration positively correlated with oil red-O-positive surface area in ApoE-deficient mice 8 weeks after inoculation with AAV5-mIL10 ($r=0.737$, $P=0.0076$).

weight, food intake, blood sugar levels, or blood pressure (data not shown).

To assess whether IL-10 causes changes in the lipoprotein profile of apoE-deficient mice, plasma lipoproteins were subjected to agarose gel electrophoresis. No differences in the patterns of lipoprotein expression were observed in AAV5-mIL10-transduced mice and AAV5-LacZ-transduced mice (data not shown).

To further understand the mechanism by which the serum cholesterol level is decreased in AAV5-mIL10-transduced mice, we evaluated cholesterol levels of HepG2 cells, human hepatocytes, incubated in the absence of lipoprotein. As shown in Figure 7, the level of cholesterol in HepG2 cells was significantly decreased by the addition of IL-10 in a dose-dependent manner. The level of intracellular cholesterol was also significantly decreased by the addition of HMG-CoA reductase inhibitor, fluvastatin, to these cells. When HepG2 cells were incubated in the presence of lipoprotein, the level of cholesterol in the conditioned medium was not decreased by the addition of IL-10 (data not shown). These data suggest that IL-10 reduces *de novo* cholesterol synthesis, but does not stimulate cholesterol uptake by hepatocytes. Furthermore, we estimated the effect of IL-10 on the expression of HMG-CoA reductase. Interestingly, IL-10 significantly decreased mRNA levels of HMG-CoA reductase ($P<0.01$), while fluvastatin, enzyme inhibitor, did not alter the expression of the enzyme itself (Figure 8).

Discussion

IL-10, a pleiotropic cytokine produced by Th2-type T cells, B cells, monocytes, and macrophages, has potent anti-inflammatory properties. The main finding of the present study is that AAV vector-mediated IL-10 gene transfer to ApoE-deficient mice following a single intramuscular administration inhibits atherosclerotic lesion formation through the inhibition of MCP-1 expression and the reduction in the level of serum cholesterol.

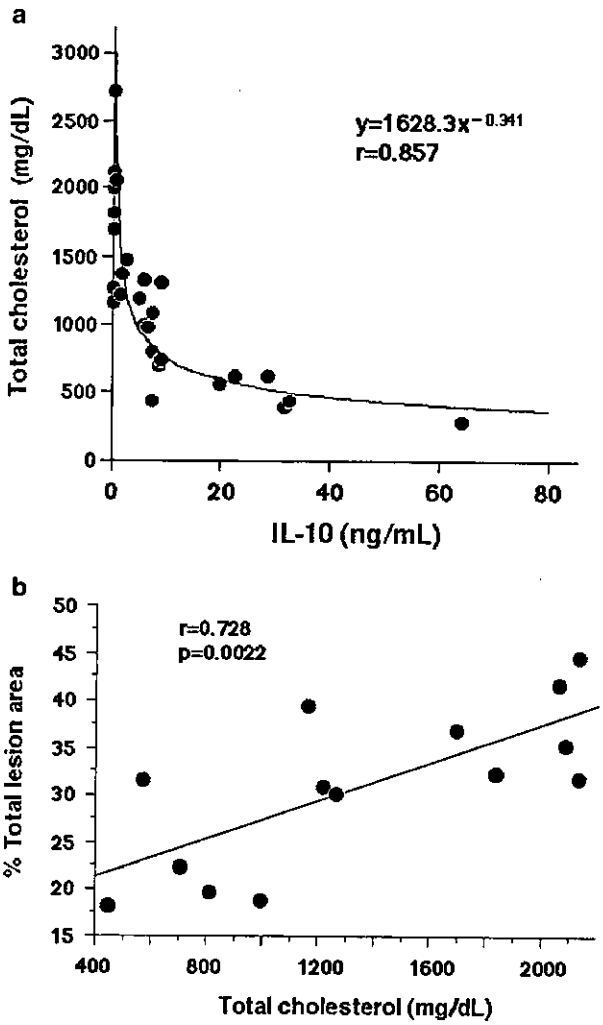

Figure 6 (a) Curve-fitting of the serum cholesterol concentration against the serum IL-10 concentration 8 weeks after inoculation of AAV5-mIL10 yielded a close fit ($r=0.857$) to a dose–response curve ($y=1628.3\times^{-0.341}$), with an EC_{50} of 5.3 ng/ml. (b) The serum cholesterol level positively correlated with atherosclerotic lesion surface area 8 weeks after inoculation with AAV5-mIL10 ($r=0.728$, $P=0.0022$).

Differentiated C2C12 cells transduced with AAV2-mIL10 were verified by Western blot analysis and enzyme-linked immunosorbent assay (ELISA) to express IL-10. The biological activity of the secreted IL-10 was also confirmed. Conditioned medium from C2C12 cells transduced with AAV2-mIL10 significantly inhibited the production of IL-6, TNF-α, and MCP-1 by J774 cells in response to LPS treatment. Based on these *in vitro* observations, we used recombinant AAV constructs to evaluate the effects of IL-10 on atherogenesis in ApoE-deficient mice. Intramuscular injection of AAV5-mIL10 into ApoE-deficient mice resulted in long-term systemic IL-10 expression. The serum IL-10 concentration was sustained at levels higher than 398.3 ± 146.6 pg/ml ($n=6$) up to 14 months after gene transfer (1×10^{12} genome copies/body).

Although double-stranded AAV genomes probably remain extrachromosomal in mouse myofibers, their tight association with chromatin allows their persistence and stable expression over periods of several months.[15–17] This particular feature of AAV vectors might be advanta-

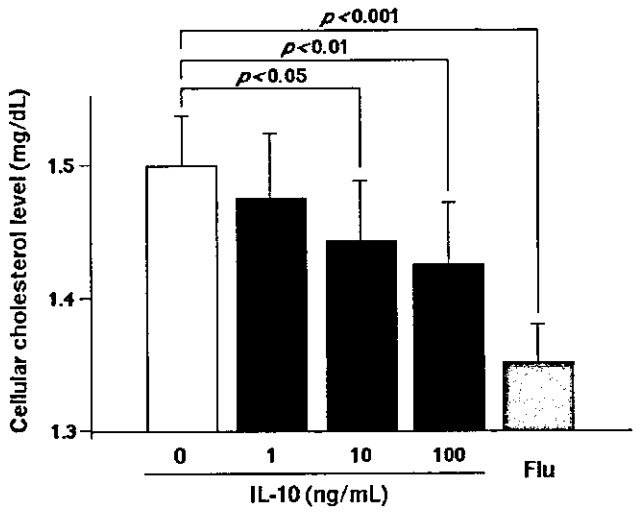

Figure 7 Cellular cholesterol level of HepG2 cells incubated in the absence of LDL cholesterol. Recombinant human IL-10 (1–100 ng/ml) or fluvastatin (10^{-5} mol/l) was added to the culture for 48 h. Data are means ± s.e.m. (n = 4).

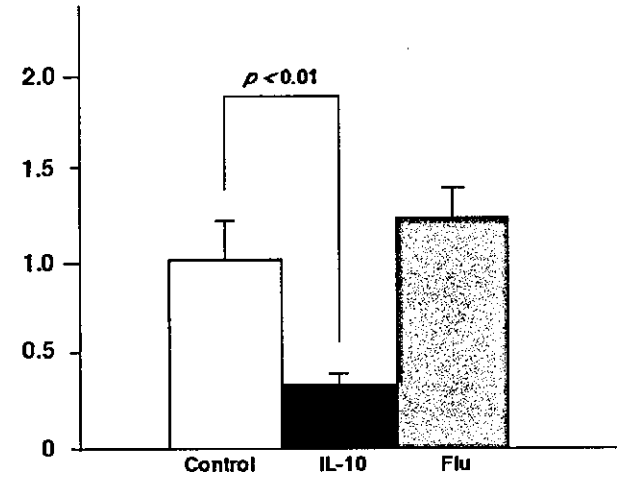

Figure 8 Relative HMG-CoA reductase expression in HepG2 treated with recombinant IL-10 as analyzed by quantitative PCR. The relative expression of the HMG-CoA reductase mRNA was determined as the ratio of the expression in HepG2 treated with IL-10 or fluvastatin to that in HepG2 incubated normally (control). Data are means ± s.e.m. (n = 3–5).

geous in investigating the effects of transgenes on chronic disease processes. Previous reports demonstrated that there was a significant difference in transgene expression by various AAV serotypes transduced into rodent muscle.[18–20] The AAV1 and AAV5 serotypes were shown to produce 100- to 1000-fold higher serum levels of transgene products, as compared to the AAV2. We selected AAV5 for use in *in vivo* experiments, since we also observed that gene transfer with AAV5 promoted a much higher level of expression of IL-10, as compared to AAV2-mediated transfer (Figure 2). However, AAV1 is reported to more efficiently transduce muscle than AAV5. Therefore, we anticipate that the use of AAV1 in future experiments would allow for a minimized vector dosage.

We focused on the effect of IL-10 on *in vivo* MCP-1 expression. MCP-1, one of the most studied members of the C–C family of chemokines, is expressed in several cell types in the arterial wall, including vascular endothelial cells, smooth muscle cells, and monocytes/macrophages, under numerous inflammatory conditions. Therefore, MCP-1 is thought to play an important role in the ongoing recruitment of monocyte–macrophages into developing lesions *in vivo*.[21] Previously, we[22] and others[21,23] reported enhanced MCP-1 expression in experimental and human atherosclerotic lesions. A role for MCP-1 in the initiation of atherogenesis was demonstrated by knockout mice in which the MCP-1 gene itself or its receptor CCR2 was inactivated.[24,25] In our study, we demonstrated that serum MCP-1 concentrations are significantly lower in IL-10-transduced mice than in control mice. In addition, we observed enhanced MCP-1 expression in the vascular wall of ApoE-deficient mice, as reported previously,[26] which was significantly inhibited by IL-10 gene transfer. Moreover, the extent of atherosclerotic lesion formation was significantly decreased in AAV5-mIL10-transduced mice, and positively correlated with serum MCP-1 concentration. These results suggest that the observed antiatherogenic effect of IL-10 is partly mediated by the inhibition of systemic and local MCP-1 expression.

We also investigated the effect of IL-10 on serum cholesterol levels. Nonlinear regression of serum cholesterol levels relative to serum IL-10 levels revealed a close correlation to a dose–effect model with an EC_{50} (5.3 ng/ml). It is well known that high cholesterol levels lead to atherogenesis in both humans and mice. Atherosclerotic lesion surface area also correlated with the serum cholesterol concentration in our study. van Exel *et al*[12] recently found a negative correlation between a low IL-10 production capacity of whole blood and total cholesterol level in humans. They speculated that high levels of IL-10 counteract the effects of TNF-α and IL-6 on lipid metabolism. This clinical observation corresponds well with our observation that the serum IL-10 concentration negatively correlates with the reduction in serum cholesterol.

Pinderski *et al*[8] found that IL-10-transgenic mice showed a decrease in atherosclerotic lesions compared to control mice. However, they found no difference in plasma cholesterol levels between the transgenic and control mice. On the other hand, Von Der Thusen *et al*[13] showed that prolonged hepatic expression of IL-10 could be achieved following intravenous adenovirus-mediated IL-10 gene transfer to LDL receptor-deficient mice. Administration of IL-10 resulted in reductions in atherosclerotic lumen stenosis and of serum cholesterol, although the cholesterol-lowering mechanism was not clarified.

We analyzed the intracellular cholesterol level of HepG2 cells cultured with acetic acid, a cholesterol substrate, in the absence of lipoprotein. This assay can measure *de novo* cholesterol synthesis, but not cholesterol uptake, in these cells. We also used fluvastatin at a dose of 10^{-5} mol/l to inhibit *de novo* cholesterol synthesis almost completely.[27] The results of these experiments suggested that IL-10, like fluvastatin, significantly inhibits the hepatic production of cholesterol. It was reported that TNF-α and IL-1 increase the levels of HMG-CoA reductase mRNA without affecting the levels of LDL receptor mRNA.[28] In other words, the increase in serum cholesterol levels observed after TNF-α and IL-1 administration is caused by an increase in hepatic cholesterol synthesis rather than a decrease in the

clearance of circulating cholesterol. These observations suggest that IL-10 might have direct effects on cholesterol metabolism through the HMG-CoA reductase pathway. We evaluated the expression of HMG-CoA reductase using quantitative PCR. As is expected, IL-10 modulated HMG-CoA reductase expression, whereas fluvastatin did not. These data suggest that the use of IL-10 in combination with statin may improve cholesterol-lowering effects and benefit the patients with atherosclerotic diseases.

Finally, we evaluated whether the downregulation of the MCP-1 was affected by the cholesterol-lowering effects of IL-10 or not. Stepwise regression analysis revealed that not only serum cholesterol but also MCP-1 concentration might be significant independent predictors of atherosclerotic lesion area. Therefore, we speculated that anti-inflammatory effect of IL-10 plays an important role in anti-atherogenic effect as well as its cholesterol-lowering effects.

In summary, AAV5-mediated IL-10-gene transfer into the skeletal muscle could introduce efficient and stable IL-10 expression, resulting in a significant antiatherogenic effects in ApoE-deficient mice. It was suggested that this effect was mediated through the anti-inflammatory and cholesterol-lowering effects of IL-10. These results indicate the presence of complex interactions between inflammation and lipid metabolism, as well as the effectiveness of anticytokine therapy using IL-10 in the treatment of atherosclerotic disease.

Materials and methods

Production of AAV vectors

Two recombinant AAV serotypes, type 2 and type 5, were used in these experiments. AAV2 and AAV5 expressing the *Escherichia coli* β-galactosidase gene under the control of the cytomegalovirus promoter (AAV2-LacZ and AAV5-LacZ) were generated with the proviral plasmids pAAV-LacZ and pAAV5-RNL, respectively. To create AAV2 and AAV5 derivatives expressing murine IL-10 (AAV2-mIL10 and AAV5-mIL10), murine IL-10 cDNA (RIKEN DNA Bank, RDB-1476) was cloned into the *Bam*HI site of pCMV to form pCMVmIL10. The IL-10 expression cassette in pCMVmIL10 was ligated as a *Not*I fragment to *Not*I-digested pAAV-LacZ and pAAV5-RNL to form the proviral plasmids pAAV2-mIL10 and pAAV5-mIL10, respectively.

AAV viral stocks were prepared according to the previously described three-plasmid transfection adenovirus-free protocol.[29] Briefly, 60% confluent 293 cells were cotransfected with the proviral plasmid, an AAV helper plasmid (pHLP19[30] for AAV2 or pAAV5RepCap[31] for AAV5), and the adenoviral helper plasmid pAdeno. The crude viral lysate was purified by two rounds of CsCl two-tier centrifugation.[32] The viral stock was titered by dot-blot hybridization with plasmid standards.

pAAV5-RNL and pAAV5-RepCap (identical to 5RepCapB) were kindly provided by Dr JA Chiorini, and pAAV-LacZ, pHLP19 and pAdeno were obtained from Avigen, Inc. (Alameda, CA, USA).

In vitro IL-10 gene transfer

The C2C12 cells were cultured in six-well plates with 2 ml Dulbecco's minimal essential medium (DMEM) containing 5% horse serum. At 8 days after plating, differentiated C2C12 cells were transduced with AAV2-mIL10 at various vector doses. The expression of IL-10 was detected by Western blot analysis after immunoprecipitation of conditioned medium and cell lysates. IL-10 concentrations were measured by ELISA (R&D Systems). To investigate the biological activities of IL-10, cultured medium from transduced C2C12 cells was added to cultured J774 cells for 30 min (final IL-10 concentration, 10 ng/ml). J774 cells were then treated with 100 ng/ml LPS and incubated for an additional 24 h. The supernatants were harvested and the concentrations of IL-6, TNF-α, and MCP-1 were quantified by ELISA (R&D Systems).

In vivo IL-10 gene transfer

All animal experiments were performed in accordance with the *Jichi Medical School Guide for Laboratory Animals*, 1993. Male ApoE-deficient mice in the C57BL/6J background (a kind gift of Dr N Maeda[33,34]) were fed on a Western-type diet containing 21% fat and 0.15% cholesterol (Harlan Teklad) from 8 weeks of age. Water and food were given *ad libitum*, and the mice were maintained on a 12-h light–dark cycle. At 8 weeks of age, ApoE-deficient mice were injected with AAV2-mIL10 (1×10^{13} genome copies/body), AAV5-mIL10 (1×10^{11}–10^{13} genome copies/body), or AAV5-LacZ (1×10^{13} genome copies/body) as 50 μl in total into two distinct sites of the anterior tibial muscle. The serum concentrations of IL-10 and MCP-1 were measured by ELISA as described above. The serum concentrations of total cholesterol were measured by HDAOS methods (Wako Pure Chemicals).

Morphometric analysis

At 8 weeks after the AAV5-mIL10 or -LacZ inoculation, the ascending aortas were removed after perfusion fixation with 4% paraformaldehyde at physiological pressure, embedded in OCT compound (Tissue-Tek), and frozen in liquid nitrogen. Atherosclerotic lesions in the aortic sinus were examined at five locations separated by 80 μm, with the most proximal site at the point where the aortic valves first appeared, and were stained with oil red-O. To quantify the aortic lesions, each image was digitized and analyzed under a microscope (Olympus) with National Institutes of Health Image software (ver. 1.61). Oil red-O-positive areas were analyzed in comparison with the total cross-sectional vessel wall area. The average value for five locations in each animal was determined.

Immunohistochemical analysis

Arterial sections were prepared from 8-week-old mice transduced with AAV5-IL-10 or AAV5-LacZ at 4 weeks old. These sections were incubated with a primary goat polyclonal antibody against mouse MCP-1 (dilution 1/250, Santa Cruz Biotechnology). Nonspecific IgG was used as a negative control. Sections were incubated with biotinylated anti-mouse secondary antibody and treated with peroxidase-conjugated streptavidin, with 3′, 3′-diaminobenzidine tetrahydrochloride as the enzyme substrate, and counterstained with hematoxylin.

Measurement of cellular cholesterol

HepG2 cells (human hepatocytes) were maintained in a 12-well plate with 1 ml of MEM containing 10% fetal bovine serum, 1% nonessential amino acids (NEAA; ICN), and 1 mmol/l sodium pyruvate at 37°C in a 5% CO_2 incubator for 5 days. The medium was then replaced with 1 ml of MEM containing 10% lipoprotein-deficient serum (LPDS; ICN), 1% NEAA, and 1 mmol/l sodium pyruvate. After 2 days later, the cells were incubated with 1 ml of MEM containing 10% LPDS, 1% NEAA and 1 mmol/l sodium pyruvate, and various concentrations (0–100 ng/ml) of recombinant human IL-10 (PeproTech) or 10^{-5} mol/l fluvastatin (Tanabe) were added to the culture. At 2 days after the treatment, the cells were incubated with 0.5 ml of MEM containing 10% LPDS, 1% NEAA, 1 mmol/l sodium pyruvate, and 2 mmol/l acetic acid for 16 h. The cellular cholesterol level was measured by an enzymatic method using Determiner TC-555 (Kyowa Medics).

mRNA analysis of HMG-CoA reductase

HepG2 cells were incubated with either recombinant human IL-10 (10 ng/ml) or fluvastatin (10^{-5} mol/l) in 10% LPDS medium for 24 h. Total RNA was isolated from the cell culture using an RNeasy Mini kit (QIAGEN) and reverse-transcribed into a single-stranded cDNA using SuperScript Preamplification System (GIBCO BRL). To estimate the expression of HMG-CoA reductase in HepG2, quantitative PCR analysis was conducted by using ABI PRISM 7700 Sequence Detection System (Applied Biosystems). The reaction was performed using the primer pairs specific for the *HMG-CoA reductase* (HMGCR-5′: GGCCCA GTTGTGCGTCTTCC and HMGCR-3′: GTTTGCTGC ATGGGCGTTGTAG) and *GAPDH* (GAPDH-5′: CGCG GGGCTCTCCAGAACATCAT and GAPDH-3′: CCAGCC CCAGCGTCAAAGGTG). Quantitative values were obtained from the threshold cycle (C_t) number that indicated exponential amplification of the PCR product. To normalize each sample, we also quantified the expression of the *GAPDH* gene. The relative target gene expression was also normalized with a calibrator (HepG2 cells without treatment of IL-10 or fluvastatin). The final result, expressed as *N*-fold differences in target gene expression relative to the *GAPDH* gene and the calibrator, was determined by the following formula: $N_{\text{target}} = 2^{\text{corrected}\Delta C_t\,(\text{GAPDH}-\text{target gene})}$. C_t values of the sample were determined by subtracting the average C_t value of the target gene from the average C_t value of the *GAPDH* gene.

Statistical analysis

Student's *t*-test or ANOVA combined with Scheffe's test was used to compare individual groups, and the Pearson's correlation test was employed to measure the linear association between two variables by using StatView (Abacus Concepts, Inc). Data are presented as means$\pm$s.e.m. A value of $P<0.05$ was considered significant.

Acknowledgements

We thank Dr John A Chiorini for providing pAAV5-RNL and pAAV5-RepCap (identical to 5RepCapB) and Avigen, Inc. (Alameda, CA, USA) for providing pAAV-LacZ, pHLP19, and pAdeno. We also thank Ms. Miyoko Mitsu for her encouragement and technical support. This study was supported in part by Research Grants from the Ministry of Education, Culture, Sports, Science and Technology; the Ministry of Health, Labor and Welfare; the Vehicle Racing Commemorative Foundation; and Mitsui Social Welfare Foundation.

References

1 The Scandinavian Simvastatin Survival Study Group. Randomised trial of cholesterol lowering in 4444 patients with coronary heart disease: the Scandinavian Simvastatin Survival Study (4S). *Lancet* 1994; **344**: 1383–1389.
2 Shepherd J *et al*. Prevention of coronary heart disease with pravastatin in men with hypercholesterolemia. West of Scotland Coronary Prevention Study Group. *N Engl J Med* 1995; **333**: 1301–1307.
3 Chen H, Ikeda U, Shimpo M, Shimada K. Direct effects of statins on cells primarily involved in atherosclerosis. *Hypertens Res* 2000; **23**: 187–192.
4 Feingold KR, Grunfeld C. Role of cytokines in inducing hyperlipidemia. *Diabetes* 1992; **41** (Suppl 2): 97–101.
5 Fiorentino DF, Bond MW, Mosmann TR. Two types of mouse T helper cell. IV. Th2 clones secrete a factor that inhibits cytokine production by Th1 clones. *J Exp Med* 1989; **170**: 2081–2095.
6 Uyemura K *et al*. Cross-regulatory roles of interleukin (IL)-12 and IL-10 in atherosclerosis. *J Clin Invest* 1996; **97**: 2130–2138.
7 Mallat Z *et al*. Expression of interleukin-10 in advanced human atherosclerotic plaques: relation to inducible nitric oxide synthase expression and cell death. *Arterioscler Thromb Vasc Biol* 1999; **19**: 611–616.
8 Pinderski Oslund LJ *et al*. Interleukin-10 blocks atherosclerotic events *in vitro* and *in vivo*. *Arterioscler Thromb Vasc Biol* 1999; **19**: 2847–2853.
9 Mallat Z *et al*. Protective role of interleukin-10 in atherosclerosis. *Circ Res* 1999; **85**: e17–e24.
10 Smith DA *et al*. Serum levels of the antiinflammatory cytokine interleukin-10 are decreased in patients with unstable angina. *Circulation* 2001; **104**: 746–749.
11 Anguera I *et al*. Elevation of serum levels of the anti-inflammatory cytokine interleukin-10 and decreased risk of coronary events in patients with unstable angina. *Am Heart J* 2002; **144**: 811–817.
12 van Exel E *et al*. Low production capacity of interleukin-10 associates with the metabolic syndrome and type 2 diabetes: the Leiden 85-Plus study. *Diabetes* 2002; **51**: 1088–1092.
13 Von Der Thusen JH *et al*. Attenuation of atherogenesis by systemic and local adenovirus-mediated gene transfer of interleukin-10 in LDLr−/− mice. *FASEB J* 2001; **15**: 2730–2732.
14 Kessler PD *et al*. Gene delivery to skeletal muscle results in sustained expression and systemic delivery of a therapeutic protein. *Proc Natl Acad Sci USA* 1996; **93**: 14082–14087.
15 Duan D *et al*. Circular intermediates of recombinant adeno-associated virus have defined structural characteristics responsible for long-term episomal persistence in muscle tissue. *J Virol* 1998; **72**: 8568–8577.
16 Bohl D *et al*. Improvement of erythropoiesis in beta-thalassemic mice by continuous erythropoietin delivery from muscle. *Blood* 2000; **95**: 2793–2798.
17 Shimpo M *et al*. AAV-mediated VEGF gene transfer into skeletal muscle stimulates angiogenesis and improves blood flow in a rat hindlimb ischemia model. *Cardiovasc Res* 2002; **53**: 993–1001.

18 Chao H *et al.* Several log increase in therapeutic transgene delivery by distinct adeno-associated viral serotype vectors. *Mol Ther* 2000; **2**: 619–623.
19 Duan D *et al.* Enhancement of muscle gene delivery with pseudotyped adeno-associated virus type 5 correlates with myoblast differentiation. *J Virol* 2001; **75**: 7662–7671.
20 Rabinowitz JE *et al.* Cross-packaging of a single adeno-associated virus (AAV) type 2 vector genome into multiple AAV serotypes enables transduction with broad specificity. *J Virol* 2002; **76**: 791–801.
21 Yla-Herttuala S *et al.* Expression of monocyte chemoattractant protein 1 in macrophage-rich areas of human and rabbit atherosclerotic lesions. *Proc Natl Acad Sci USA* 1991; **88**: 5252–5256.
22 Seino Y *et al.* Expression of monocyte chemoattractant protein-1 in vascular tissue. *Cytokine* 1995; **7**: 575–579.
23 Nelken NA, Coughlin SR, Gordon D, Wilcox JN. Monocyte chemoattractant protein-1 in human atheromatous plaques. *J Clin Invest* 1991; **88**: 1121–1127.
24 Gu L *et al.* Absence of monocyte chemoattractant protein-1 reduces atherosclerosis in low density lipoprotein receptor-deficient mice. *Mol Cell* 1998; **2**: 275–281.
25 Boring L, Gosling J, Cleary M, Charo IF. Decreased lesion formation in CCR2−/− mice reveals a role for chemokines in the initiation of atherosclerosis. *Nature* 1998; **394**: 894–897.
26 Rayner K, Van Eersel S, Groot PH, Reape TJ. Localisation of mRNA for JE/MCP-1 and its receptor CCR2 in atherosclerotic lesions of the ApoE knockout mouse. *J Vasc Res* 2000; **37**: 93–102.
27 Mascaro C *et al.* Sterol regulatory element binding protein-mediated effect of fluvastatin on cytosolic 3-hydroxy-3-methylglutaryl-coenzyme A synthase transcription. *Arch Biochem Biophys* 2000; **374**: 286–292.
28 Hardardottir I *et al.* Effects of TNF, IL-1, and the combination of both cytokines on cholesterol metabolism in Syrian hamsters. *Lymphokine Cytokine Res* 1994; **13**: 161–166.
29 Matsushita T *et al.* Adeno-associated virus vectors can be efficiently produced without helper virus. *Gene Therapy* 1998; **5**: 938–945.
30 Okada T *et al.* Development and characterization of an antisense-mediated prepackaging cell line for adeno-associated virus vector production. *Biochem Biophys Res Commun* 2001; **288**: 62–68.
31 Chiorini JA, Kim F, Yang L, Kotin RM. Cloning and characterization of adeno-associated virus type 5. *J Virol* 1999; **73**: 1309–1319.
32 Okada T *et al.* Adeno-associated viral vector-mediated gene therapy of ischemia-induced neuronal death. *Methods Enzymol* 2002; **346**: 378–393.
33 Zhang SH, Reddick RL, Piedrahita JA, Maeda N. Spontaneous hypercholesterolemia and arterial lesions in mice lacking apolipoprotein E. *Science* 1992; **258**: 468–471.
34 Ishibashi S *et al.* The two-receptor model of lipoprotein clearance: tests of the hypothesis in "knockout" mice lacking the low density lipoprotein receptor, apolipoprotein E, or both proteins. *Proc Natl Acad Sci USA* 1994; **91**: 4431–4435.